JGP Journal of General Physiology

ARTICLE

N-terminal truncated cardiac troponin I enhances Frank-Starling response by increasing myofilament sensitivity to resting tension

Han-Zhong Feng[1], Xupei Huang[2], and Jian-Ping Jin[1]

Cardiac troponin I (cTnI) of higher vertebrates has evolved with an N-terminal extension, of which deletion via restrictive proteolysis occurs as a compensatory adaptation in chronic heart failure to increase ventricular relaxation and stroke volume. Here, we demonstrate in a transgenic mouse model expressing solely N-terminal truncated cTnI (cTnI-ND) in the heart with deletion of the endogenous cTnI gene. Functional studies using ex vivo working hearts showed an extended Frank-Starling response to preload with reduced left ventricular end diastolic pressure. The enhanced Frank-Starling response effectively increases systolic ventricular pressure development and stroke volume. A novel finding is that cTnI-ND increases left ventricular relaxation velocity and stroke volume without increasing the end diastolic volume. Consistently, the optimal resting sarcomere length (SL) for maximum force development in cTnI-ND cardiac muscle was not different from wild-type (WT) control. Despite the removal of the protein kinase A (PKA) phosphorylation sites in cTnI, β-adrenergic stimulation remains effective on augmenting the enhanced Frank-Starling response of cTnI-ND hearts. Force–pCa relationship studies using skinned preparations found that while cTnI-ND cardiac muscle shows a resting SL–resting tension relationship similar to WT control, cTnI-ND significantly increases myofibril Ca^{2+} sensitivity to resting tension. The results demonstrate that restrictive N-terminal deletion of cTnI enhances Frank-Starling response by increasing myofilament sensitivity to resting tension rather than directly depending on SL. This novel function of cTnI regulation suggests a myofilament approach to utilizing Frank-Starling mechanism for the treatment of heart failure, especially diastolic failure where ventricular filling is limited.

Introduction

Troponin I (TnI) is the inhibitory subunit of the troponin complex in striated muscles and plays a central role in the Ca^{2+}-regulation of contraction and relaxation (Sheng and Jin, 2016). Three muscle type TnI isoform genes have evolved in vertebrates, of which cardiac TnI (cTnI) is specifically expressed in postnatal and adult hearts (Jin, 1996). Diverged from skeletal muscle TnIs, cTnI of tetrapods has an N-terminal extension (Chong and Jin, 2009; Rasmussen et al., 2022) that contains β-adrenergic–regulated protein kinase A (PKA) phosphorylation sites at Ser^{23} and Ser^{24}. Posttranslational modification of cTnI plays an important role in regulating heart functions. PKA phosphorylation of cTnI reduces myofilament Ca^{2+} affinity (Kranias and Solaro, 1982; Zhang et al., 1995) and facilitates the relaxation of cardiac muscle (Robertson et al., 1982; Zhang et al., 1995; Kentish et al., 2001; Wolska et al., 2002).

Another posttranslational modification of cTnI is by restrictive proteolysis to selectively remove the N-terminal extension while preserving the conserved core structure (Yu et al., 2001). Low levels of N-terminal-truncated cTnI (cTnI-ND) are present in normal cardiac muscle, which increases during physiological adaptation (Yu et al., 2001) and in Gsα deficient failing hearts (Feng et al., 2008b). Transgenic mouse hearts over-expressing cTnI-ND produced increased ventricular relaxation, an effect similar to that of PKA phosphorylation at N-terminal Ser^{23}/Ser^{24} of intact cTnI (Barbato et al., 2005), demonstrating that cTnI-ND is an adaptation to compensate for impaired diastolic cardiac function especially when PKA phosphorylation of cTnI is blunted in failing hearts (McConnell et al., 1998; Zakhary et al., 1999).

The effect of cTnI-ND on increasing myocardial relaxation was further demonstrated by expressing cTnI-ND to correct the diastolic dysfunction caused by a restrictive cardiomyopathy

[1]Department of Physiology and Biophysics, University of Illinois at Chicago School of Medicine, Chicago, IL, USA; [2]Charles E. Schmidt College of Medicine, Florida Atlantic University, Boca Raton, FL, USA.

Correspondence to J.-P. Jin: jpjin@uic.edu.

mutation (R193H) of cTnI in the hearts of double transgenic mice (Li et al., 2010). By improving ventricular relaxation and diastolic filling to enhance cardiac function through the inotropic effect of Frank-Starling response that is diminished in failing hearts (Schwinger et al., 1994), the compensatory adaptation by cTnI-ND modification demonstrates an attractive molecular mechanism for the treatment of diastolic heart failure, i.e., heart failure with preserved ejection fraction (HFpEF), a condition involving approximately half of heart failure patients but having no effective treatment available (Zile and Brutsaert, 2002; Yancy et al., 2013).

Frank-Starling response of the heart is the fundamental mechanism to increase stroke volume as ventricular end diastolic volume increases (Shiels and White, 2008). After more than a century of research, the molecular basis of Frank-Starling mechanism is still not fully understood. Our previous studies have demonstrated the effect of overexpressing cTnI-ND to replace ∼70% of intact cTnI on increasing ventricular relaxation and stroke volume (Barbato et al., 2005; Feng et al., 2008b). To more specifically investigate how cTnI-ND enhances Frank-Starling response of the heart, we employed a mouse model from crossing cTnI-ND transgenic mice with endogenous cTnI gene (*Tnni3*) knockout (KO) mice to express solely cTnI-ND in postnatal hearts (Feng et al., 2009) in multi-level functional studies. From quantitative analyses using in vivo echocardiogram, ex vivo working hearts and skinned cardiac muscle contractility, the results show that cTnI-ND,*Tnni3*$^{-/-}$ hearts respond to increases in preload with higher contractile and relaxation velocities and larger stroke volume than that of wild-type (WT) hearts, whereas the left ventricular end diastolic volume and optimal resting sarcomere length (SL) of cardiac muscle were not increased. Force–pCa (-log of molar [Ca^{2+}]) relationship in skinned cTnI-ND,*Tnni3*$^{-/-}$ cardiac muscle strips showed steeper response of increasing Ca^{2+} sensitivity to resting tension than WT control. The finding that cTnI-ND enhances Frank-Starling response without increasing left ventricular end diastolic volume or pressure demonstrates a novel mechanism to increase the sensitivity of cardiac myofilaments to resting tension, suggesting a myofilament approach to utilize Frank-Starling mechanism for the treatment of heart failure, especially diastolic heart failure where limited ventricular end diastolic volume underlies the pathophysiology.

Materials and methods

Animal model

All animal procedures were carried out using protocols approved by the Institutional Animal Care and Use Committees of University of Illinois at Chicago and Florida Atlantic University and were conducted in accordance with the National Institutes of Health Guide for the Care and Use of Laboratory Animals.

cTnI-ND,*Tnni3*$^{-/-}$ double transgenic mice were produced as previously described (Feng et al., 2009) by rescuing the postnatal lethality of *Tnni3* gene-deleted mice (Huang et al., 1999) with a transgene allele that postnatally expresses cTnI-ND (Barbato et al., 2005) driven by the α-myosin heavy chain (α-MHC) promoter (Subramaniam et al., 1993). The cTnI-ND transgenic and the *Tnni3*$^{-/-}$ mice used to generate the double transgenic line were both in full C57BL/6J background assured by more than nine generations of back-cross breeding with WT C57BL/6J mice from Jackson Labs. The full C57BL/6J genetic background of cTnI-ND,*Tnni3*$^{-/-}$ double transgenic mice allows us to use age- and sex-matched WT C57BL/6J mice from Jackson Labs as controls. Genotyping of the offspring was done using PCR on genomic DNA isolated from tissue biopsies as described previously (Feng et al., 2009). The absence of intact cTnI and replacement with cTnI-ND at normal stoichiometry in adult cardiac muscle of the double transgenic mice were verified using Western blotting of total protein extract (Feng et al., 2009).

Ex vivo mouse working heart preparation and functional measurements

Cardiac function was measured in ex vivo working hearts (Feng et al., 2008a) prepared from 3–4-mo-old male cTnI-ND,*Tnni3*$^{-/-}$ double transgenic and WT C57BL/6J mice. 30 min after i.p. injection of 100 units of heparin, the mouse was anesthetized with pentobarbital sodium (100 mg/kg body weight, i.p.) and the heart was rapidly isolated with the large vessels attached. A blunted 18-gauge needle 6 mm long with thinned wall was used to cannulate the aorta to establish retrograde perfusion of a modified Krebs-Hensileit buffer aerated with 95% O_2, 5%CO_2 at 37°C. The buffer consists of 118 mM NaCl, 4.7 mM KCl, 2.25 mM $CaCl_2$, 2.25 mM $MgSO_4$, 1.2 mM KH_2PO_4, 0.32 mM EGTA, 25 mM $NaHCO_3$, 15 mM D-glucose, and 2 mM sodium pyruvate, pH 7.4 at 37°C. A blunted 16-gauge needle was used to cannulate pulmonary vein for antegrade perfusion through the left atrium. Venae cavae were sutured and a beveled PE-50 tubing was used to cannulate the pulmonary artery to collect coronary effluent. The heart was then switched to working mode by opening the left atrial perfusion. The perfusion buffer was not recycled, avoiding complicating effect of metabolic products.

A 30-gauge needle was used to puncture the left ventricle from the apex to make a path for inserting a 1.2 French pressure-volume (P-V) catheter (Model 898B; Scisense) calibrated for pressure and volume readings at 37°C. Aortic pressure was measured using an MLT844 pressure transducer. A 0.5-ml air bubble was placed in the compliance chamber to mimic in vivo aortic compliance. The aortic flow was recorded in real time by calibrated drop counting using a pair of electrodes feeding to a Powerlab/16 SP digital data archiving system (AD Instruments). Coronary flow from the pulmonary artery was recorded using another pair of electrodes. Cardiac output was calculated as the sum of aortic and coronary flows.

Under supraventricular pacing using an isolated stimulator (A365; World Precision Instrument) through a pair of microplatinum electrodes attached to the surface of right atrium, the heart rate was controlled at 480 beats per minute (bpm) at baseline and 540 bpm during isoproterenol (ISO) treatment. Baseline function of the ex vivo mouse working hearts was measured for left ventricular (LV) pressure, maximum rates of LV pressure development (±dP/dt) and LV stroke volume.

After stabilization at preload of 10 mmHg and afterload of 55 mmHg (the default condition for Krebs buffer perfused mouse working hearts) and recording the baseline functions, the

functional response to preload was examined at left atrium perfusion pressures of 3, 5, 8, 10, 12.5, 15, and 20 mmHg for the effect of cTnI-ND on Frank-Starling response. The assay was then repeated in the presence of 10 nM ISO after a restabilization period at 10 mmHg preload and 55 mmHg afterload (Feng et al., 2008b).

At the end of the functional measurements, all hearts studied were weighed and samples of ventricular muscle processed for Western blot studies including the use anti-cTnI antibody to confirm the cTnI-ND,*Tnni3*$^{-/-}$ and WT genotypes.

SDS-polyacrylamide gel electrophoresis (PAGE) and Western blotting

Mouse ventricular muscle immediately collected after euthanasia or after working heart experiments was homogenized in SDS-gel sample buffer containing 2% SDS and heated at 80°C for 5 min. Resolved on 14% SDS-gel with acrylamide:bisacrylamide ratio of 180:1, intact cTnI and cTnI-ND were detected using a monoclonal antibody (mAb) TnI-1 as described previously (Feng et al., 2009). Expression of cardiac troponin T (TnT) was examined using mAb CT3 as described (Feng et al., 2009). Western blotting of SERCA2a was done using mAb 1C10G10 (a gift from Dr. Steven Cala, Wayne State University, Detroit, MI, USA).

Cardiac muscle samples were run on 15% SDS-gel with acrylamide:bisacrylamide ratio of 29:1 to examine phospholamban and Ser^{16}-phosphorylated phospholamban. The protein extract of mouse heart tissue was heated to 80°C and immediately loaded to SDS-gel to minimize the formation of phospholamban pentamer. Total phospholamban was detected using mAb 2D12 (Wu et al., 2016), and Ser^{16}-phosphorylated phospholamban was quantified using a rabbit polyclonal anti-phospho-phospholamban antibody (Upstate Biotechnology).

ISO treatment in vivo and Pro-Q diamond staining of total phosphoproteins

3-mo-old cTnI-ND,*Tnni3*$^{-/-}$ and WT C57BL/6J mice were anesthetized with pentobarbital (100 mg/kg body weight, i.p.). ISO was administrated i.p. at 2 mg/kg body weight. Increases in heart rate were monitored using surface electrocardiography to indicate the effect of ISO. After the ISO effect became stable, the chest was opened to quickly isolate the heart and euthanize the mouse. LV cardiac muscle was rapidly collected, immediately frozen in liquid nitrogen, and stored at −80°C. The frozen samples were rapidly homogenized in SDS-gel sample buffer without thawing and heated at 80°C for 5 min for SDS-PAGE and Pro-Q Diamond stain of total phosphoproteins. As described previously (Feng et al., 2008b), SDS-gels were prefixed in 50% methanol/10% acetic acid for 45 min and kept in fresh fixer overnight. After washing three times with deionized water for 10 min each, the gels were stained for 90 min in a dark container with Pro-Q Diamond reagent (Invitrogen). After destaining in 20% acetonitrile and 50 mM sodium acetate, pH 4.0, for three changes of 30 min each, the gels were washed for 5 min twice in deionized water and imaged using a Typhoon 9410 fluorescence scanner (GE Healthcare) with excitation at 532 nm and recording the emission at 560 nm.

Agarose SDS-gel electrophoresis

cTnI-ND,*Tnni3*$^{-/-}$ and WT C57BL/6J mouse hearts were examined for titin in 1% agarose SDS mini gel using a published protocol (Warren et al., 2003) with some modifications. Frozen muscle tissue was weighed and mechanically homogenized at 3,000 rpm using a Pro 200 homogenizer in a sample buffer containing 8 M urea, 2 M thiourea, 3% SDS, 75 mM dithiothreitol (DTT), 0.03% bromophenol blue, and 0.05 M Tris-HCl, pH 6.8 in 1:40 ratio (W(mg)/V(μL)). The samples were heated at 60°C for 5 min, vortexed, and centrifuged at 20,000 × *g* for 5 min. The clarified samples were loaded to the gels or aliquoted and stored at −80°C for later use.

The gel was casted in Bio-Rad Mini gel format (8 × 10 cm and 1.5 mm thick). A 0.5-cm plug of 8% polyacrylamide gel was first made at the bottom with a water overlay for flat interface. The casting assembly was then preheated to 65°C before pouring the resolving gel solution contains 1% (w/v) Sea Kem Gold agarose (Biowhittaker Cell Biology Products), 30% (v/v) glycerol, 50 mM Tris-base, 0.384 M glycine, and 0.1% (w/v) SDS prepared by boiling in a microwave oven.

After the gel solidified at room temperature, vertical electrophoresis was run with 50 mM Tris-base, 0.384 mM glycine, and 0.1% SDS in the lower buffer chamber, and the same buffer plus 10 mM 2-mercaptoethanol in the upper buffer chamber. The gel was run at constant 100 V for 3 h in an ice box until the dye front reached to the bottom of the polyacrylamide gel plug. The gel was stained using Coomassie blue R-250 and destained in standard methanol/acetic acid destaining solution with gentle shaking until the background cleared. A duplicate gel was examined using Pro-Q phosphorprotein stain as above.

Echocardiography

2-mo-old female cTnI-ND,*Tnni3*$^{-/-}$ and WT C57BL/6J mice were used in echocardiography study. The use of female mice to measure in vivo cardiac function was based on the consideration that they were under less stress than males when housed with multiple mice per case. Testing at the young age also minimizes chronic compensatory effects. Echocardiography studies were performed using a Vevo 770 rodent imaging system (VisualSonics) as described previously (Li et al., 2013). All measurements were done by an examiner blinded for the mouse genotypes. The mice were anesthetized with 1.2% isoflurane inhalation and placed on a heating pad to maintain body temperature at 37°C. Hair on the precordial region was removed using Nair lotion hair remover, and the region was covered with ultrasound transmission gel (Aquasonic, Parker Laboratory). Short-axis M-mode images during diastole and systole were obtained to measure ventricular structure and dimension. Transmitral blood flow was measured with the Pulse Doppler and diastolic mitral annular velocity was measured with the Tissue Doppler methods. After measurement of baseline functions, ISO was administrated (0.2 mg/kg body weight, i.p.) and the measurement was repeated for β-adrenergic response. The data and images were saved and analyzed using the Advanced Cardiovascular Package Software (FUJI Visual Sonics).

Measurement of optimal SL of mouse LV papillary muscle

cTnI-ND,*Tnni3*$^{-/-}$ and C57BL/6J WT control mice were heparinized and anesthetized as above. Hearts were isolated and pinned on a pad of silicon rubber affixed in a dissection dish, immerged in a continuous flow of Kreb's solution gassed with 95% O_2, 5% CO_2 at room temperature. The left ventricle was opened, and the papillary muscles were removed together with the mitral valve tendon and a piece of ventricular wall tissue at the base using a pair of sharp microscissors. The isolated papillary muscle was mounted with sutures horizontally in a 2-ml flow bath in connection to a force transducer (300B LR, Aurora Scientific Instrument). The temperature of the perfusing solution was controlled at 22 ± 0.5°C using a feedback thermocontroller. Field electrical stimulation was applied every 10 s at 10 V in 4 ms pulses to induce contractions. Maximum isometric force development was achieved by gradually increasing the muscle length to identify the optimal length of active force production.

After the maximum force development became stable, the papillary muscle at resting state was fixed at the optimal length in situ on the apparatus with 3.7% formalin in phosphate buffered saline (PBS), pH 7.4, at room temperature for 30 min. No change in resting tension was observed during the fixation, indicating a maintained structural state representing the optimal resting muscle length for the maximum development of isometric active force. The fixed papillary muscle was removed from the apparatus and stored in 3.7% formalin at 4°C overnight. After dehydration for 48 h with three changes of 30% sucrose in PBS, pH 7.4, at 4°C (after the muscle tissue sank to the bottom of the tube), the papillary muscles were embedded in Optimal Cutting Temperture (O.C.T.) compound and flash frozen in liquid nitrogen. Frozen sections were cut at 5 µm thickness along the long axis using a cryostat, processed, and processed for H&E

Table 1. **cTnI-ND,*Tnni3*$^{-/-}$ double transgenic mice have normal heart weight**

	WT (n = 6)	cTnI-ND,*Tnni3*$^{-/-}$ (n = 9)
Body weight (g)	28.37 ± 0.31	29.79 ± 1.51
Heart weight (mg)	155.55 ± 4.77	151.87 ± 4.89
Heart weight/body weight (mg/g)	5.48 ± 0.17	5.23 ± 0.07

Body weight, heart weight, and heart weight/body weight ratio of cTnI-ND,*Tnni3*$^{-/-}$ double transgenic and age-matched WT C57BL/6J control mice at 3–4 mo old did not show significant difference. The values are mean ± SEM.

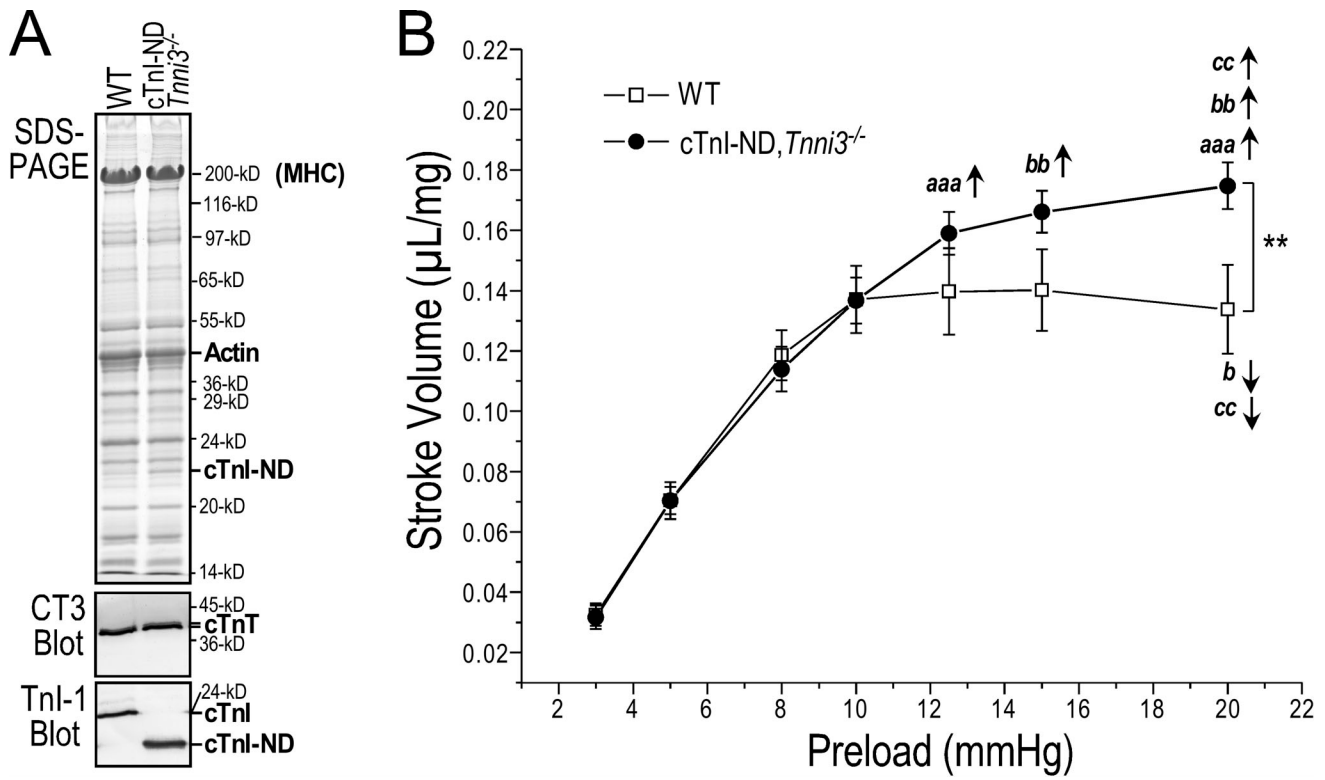

Figure 1. **cTnI-ND,*Tnni3*$^{-/-}$ex vivo working hearts show extended Frank-Starling response as compared to WT control. (A)** The SDS-gel and mAb TnI-1 Western blot show the expression of solely cTnI-ND in the heart of adult cTnI-ND,*Tnni3*$^{-/-}$ double transgenic mice. Age-matched WT C57BL/6J mouse heart was examined as control. Normal expression of cTnT in cTnI-ND,*Tnni3*$^{-/-}$ mouse heart is shown by the mAb CT3 blot. MHC, myosin heavy chain. **(B)** The Frank-Starling response curves show that the stroke volume of cTnI-ND,*Tnni3*$^{-/-}$ mouse hearts normalized to heart weight continued to increase when preload was raised above 10 mmHg whereas it was plateaued in WT hearts. The values are mean ± SEM. n = 5–6 mice in WT and 8–9 mice in cTnI-ND,*Tnni3*$^{-/-}$ groups. *P < 0.05 and **P < 0.05 vs. WT at preload of 10–20 mmHg in two-way ANOVA with post-hoc method of Tukey test; ^{aaa}P < 0.001 vs. stroke volume at 10 mmHg preload; ^{b}P < 0.05 and ^{bb}P < 0.01 vs. stroke volume at 12.5 mmHg preload; ^{cc}P < 0.01 vs. stroke volume at 15 mmHg preload in paired Student's t test. ↑ and ↓ indicate increase and decrease in the comparisons.

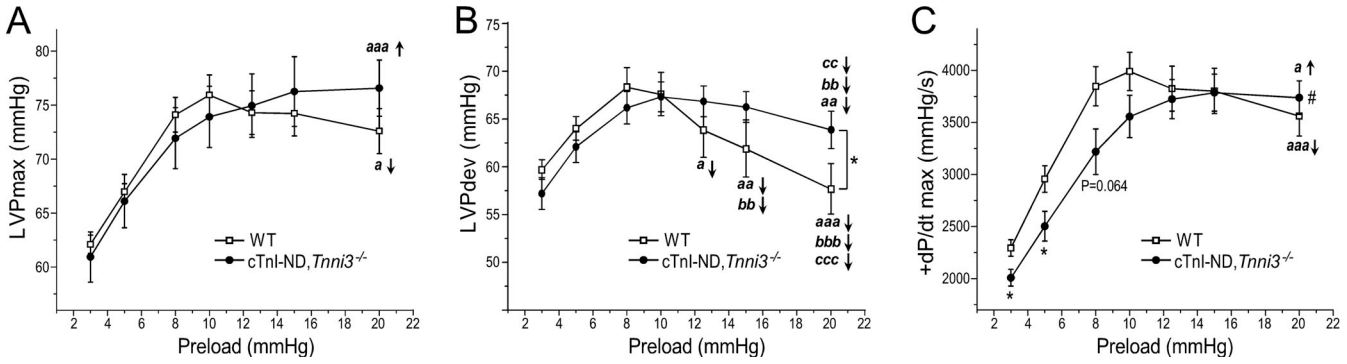

Figure 2. **cTnI-ND,*Tnni3*$^{-/-}$ hearts show higher positive systolic response to increase of preload than WT control. (A)** WT and cTnI-ND,*Tnni3*$^{-/-}$ hearts both showed positive response of LVP_{max} to increase of preload from 3 to 10 mmHg. cTnI-ND,*Tnni3*$^{-/-}$ hearts maintained high LVP_{max} at higher preload of 15–20 mmHg, whereas WT controls showed decreases. **(B)** This trend was confirmed by measuring LVP_{dev} (LVP_{max} − LVP_{min}). **(C)** The LV maximum systolic velocity (+dP/dt_{max}) of cTnI-ND,*Tnni3*$^{-/-}$ and WT hearts both positively responded to increase of preload from 3 to 10 mmHg while cTnI-ND,*Tnni3*$^{-/-}$ hearts had detectably lower + dP/dt_{max} than that of WT hearts. The difference diminished when preload was above 10 mmHg. At higher preload, +dP/dt_{max} of WT hearts became lower than that at 10 mmHg whereas it continued rising in cTnI-ND,*Tnni3*$^{-/-}$ hearts. The values are mean ± SEM. *n* = 5–6 mice in WT and 8–9 mice in cTnI-ND,*Tnni3*$^{-/-}$ groups. $^{\#}P < 0.05$ vs. WT in Student's t test. $^{*}P < 0.05$ vs. WT in two-way ANOVA with post-hoc method of Tukey's test at preload from 10 to 20 mmHg; $^{a}P < 0.05$, $^{aa}P < 0.01$, and $^{aaa}P < 0.001$ vs. that at 10 mmHg preload; $^{bb}P < 0.01$ and $^{bbb}P < 0.001$ vs. that at 12.5 mmHg preload; $^{cc}P < 0.01$ and $^{ccc}P < 0.001$. ↑ and ↓ indicate increase and decrease in the comparisons.

staining to measure the average length of 10 or more sarcomeres in each image under a light microscope.

Measurement of resting/slack SL in isolated cardiomyocytes

Hearts of cTnI-ND,*Tnni3*$^{-/-}$ and WT C57BL/6J control mice were cannulated through aorta as above and retrograde-perfused with 165 unit/ml collagenase (Worthington) in the presence of 25 µM $CaCl_2$ in Kreb's solution containing 120 mM NaCl, 5.4 mM KCl, 1.2 mM $MgSO_4$, 1.2 mM NaH_2PO_4, 10 mM 2,3-butanedione monoxime (BDM), 5.6 mM glucose, 20 mM $NaHCO_3$, and 5 mM taurine, pH 7.4, aerated with 95% O_2, 5% CO_2 at 37°C at a constant flow of 2 ml/min (Wei and Jin, 2015). The collagenase perfusion was stopped at ∼30 min when the ventricular tissue became pale. The digested ventricular muscle was transferred to a stopping solution of Kreb's buffer containing 25 µM $CaCl_2$ and 10% fetal bovine serum. Cardiomyocytes were dissociated by briefly tattering of the tissue using a pair of forceps and repeated pipetting with a large pore pipette. The isolated cardiomyocytes were filtered through a 200-mesh screen and collected by centrifugation at 200 × *g* for 1 min before resuspended in Kreb's buffer containing 50 µM $CaCl_2$ and 5% fetal bovine serum. Ca^{2+} was then gradually restored to physiological level (to 0.1 mM at 6 min, 0.2 mM at 8 min, 0.5 mM at 12 min, and 1 mM at 16 min). Images of the isolated cardiomyocytes were photographed at 25°C in an environmentally controlled heating chamber (TC-324B; Warner Instrument) mounted on an inverted microscope to measure the resting/slack SL in the absence of external load.

Contractility of skinned papillary muscle strips

Using the cryosectioning method previously described (Feng and Jin, 2020), we studied the Ca^{2+}-activated force production of permeabilized of cTnI-ND,*Tnni3*$^{-/-}$ and WT C57BL/6J control mouse cardiac muscles at various SLs. Briefly, 3–4-mo-old male mice were anesthetized using isoflurane as above and the hearts removed to isolate the LV papillary muscles. The papillary muscle was rapidly frozen with O.C.T. compound in liquid nitrogen for cryosectioning at −20°C into 120–150 µm wide, 35-µm-thick longitudinal strips. The frozen muscle strips were transferred into the liquid form of a relaxation buffer (40 mM N,N-bis(2-hydroxyethyl)-2-aminoethanesulfonic acid [BES] sodium, 10 mM EGTA, 6.86 mM $MgCl_2$, 5.96 mM ATP, 1 mM DTT, 3.28 mM K-propionate, 33 mM creatine phosphate, 200 U/ml creatine kinase, pH 7.0, and a cocktail of protease inhibitors) containing 50% glycerol (v/v) for incubation at −20°C for 24 h to restore the frozen muscle into native soft tissue with preserved myofibril and sarcomere structures. The uniformly sectioned thin papillary muscle strips assure effective perfusion and have similar cross-sectional area for accurate normalization of passive and active tension measurements and comparison between samples.

Papillary muscle strips with cardiomyocytes parallelly organized along the long axis were selected under a high power dissecting microscope to mount with aluminum T-clips between a lever arm length controller (ASI, 322C) and a force transducer (ASI, 403A) in a chamber of an eight-chamber thermal controlled stage (ASI, 802D) containing a skinning buffer (the relaxation buffer plus 1% Triton X-100) and incubated at 4–6°C for 30 min. Sarcomeric striations were imaged at 200× magnification using a digital camera.

Contractility studies were carried out at 15°C in 40 mM BES, 6.64 mM $MgCl_2$, 6.23 mM ATP, 1 mM DTT, 2.09 mM K-propionate, 33 mM creatine phosphate, 200 U/ml creatine kinase, protease inhibitor cocktail, 10 mM EGTA, pH 7.0, and 10 mM Ca-EGTA (formulated for a series of free $[Ca^{2+}]$ calculated as described [Fabiato and Fabiato, 1979; Lee et al., 2010] to measure isometric force–pCa relationship at various SLs through an AD interface (ASI, 604C) and computer software (ASI, ASI-600) and fitted using a Hill equation: *F*/*F*max (relative tension) = $[Ca^{2+}]^n$ / (K + $[Ca^{2+}]^n$), where *n* is the Hill coefficient, to calculate the half-maximal activation, pCa50, as (−logK)/*n*

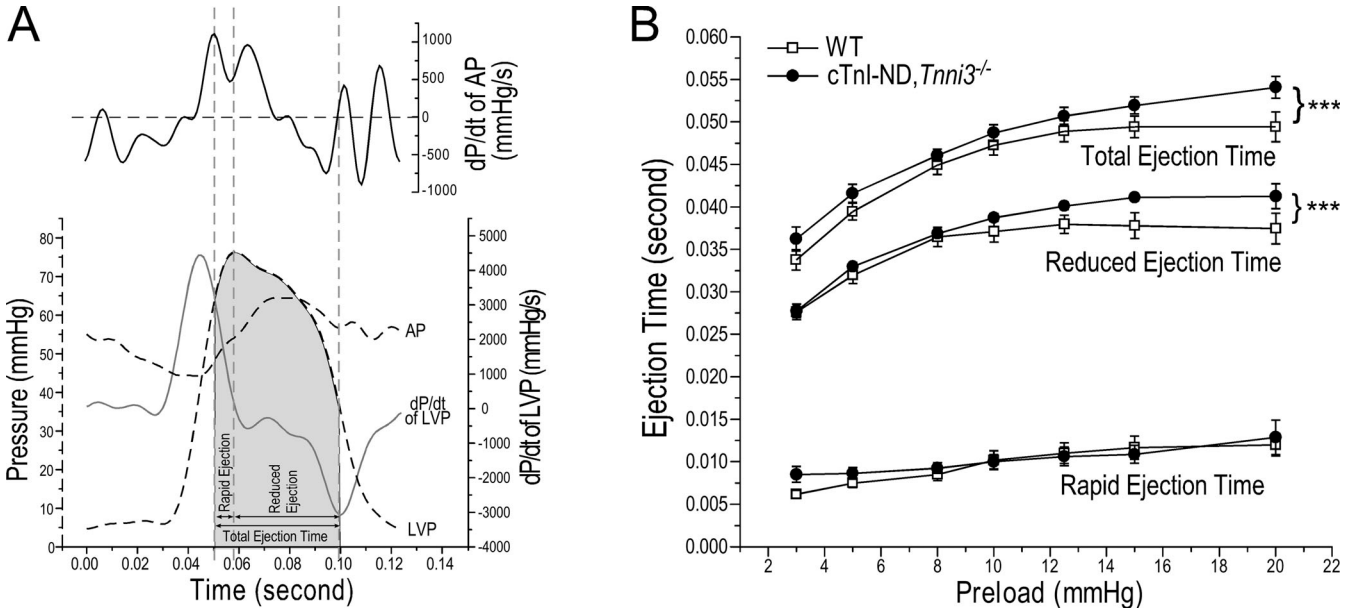

Figure 3. **cTnI-ND,*Tnni3*$^{-/-}$ hearts have longer LV ejection time at high preload. (A)** Determination of LV ejection time of ex vivo working heart from the dP/dt of aortic pressure (AP) development curves. The first and highest peak of +dP/dt of AP development indicates the full opening of the aortic valve, which marks the beginning of the ejection phase. The end point of AP descending when the dP/dt of AP development = 0 indicates the closing of the aortic valve and the end of LV ejection. The total duration of LV ejection is divided at the peak of LVP into the rapid and reduced ejection phases. **(B)** LV total ejection time increased in both cTnI-ND,*Tnni3*$^{-/-}$ and WT hearts when preload was increased, which was longer in cTnI-ND,*Tnni3*$^{-/-}$ hearts especially at preloads above 12.5 mmHg due to continued positive response vs. the plateau in WT hearts. The duration of rapid ejection phase was similar in the two groups while cTnI-ND,*Tnni3*$^{-/-}$ hearts exhibited a trend of longer time at low preloads. The reduced ejection phase was longer in cTnI-ND,*Tnni3*$^{-/-}$ hearts than that in WT hearts at the higher preloads of 10–20 mmHg. *n* = 6 mice in WT and 9 mice in cTnI-ND,*Tnni3*$^{-/-}$ groups. Values are mean ± SEM. ***P < 0.001 vs. WT in two-way ANOVA with post-hoc method of Tukey's test.

(Lee et al., 2010). At the end of each experiment, the muscle strip with T-clips was recovered and stored at −80°C for protein analysis.

Data analysis

Densitometry quantitation of protein bands in SDS-gel and Western blot was performed using ImageJ software on images scanned at 600 dpi. While one mouse heart may provide multiple strips for skinned fiber studies, the *n* numbers used in statistical test are the number of mice. Statistical analysis was done using one-way ANOVA, two-way ANOVA, or Student's *t* test as noted in the figure legends. When multiple cells or muscle strips were analyzed per mouse, the data from one mouse are averaged for statistical analysis with the number of mice as *n*.

Results

cTnI-ND,*Tnni3*$^{-/-}$ mouse hearts show extended Frank-Starling response

The α-MHC promoter-driven expression of cTnI-ND in postnatal cardiac muscle effectively rescued the lethal phenotype of endogenous cTnI gene deletion to produce adult cardiac muscle containing solely cTnI-ND as a definitive experimental system for investigating the physiological functions of cTnI-ND without the influence of endogenous intact TnI (Fig. 1 A). Heart mass indexed as the ratio of heart weight to body weight showed no significant difference between cTnI-ND,*Tnni3*$^{-/-}$ and WT C57BL/6J control mice at 3–4 mo of age, precluding hypertrophy or loss of cardiomyocytes (Table 1). The results confirm the nature of the restrictive truncation of the N-terminal extension of cTnI as a non-destructive adaptation in vivo (Yu et al., 2001).

With heart rates paced at a physiological level (480 bpm), the ex vivo mouse working heart studies of intrinsic cardiac functions in the absence of neurohumoral influence showed that when preload increased from 3 to 10 mmHg, cTnI-ND,*Tnni3*$^{-/-}$ hearts produced a positive Frank-Starling response in stroke volumes similar to that of WT C57BL/6J hearts. When preload was further increased from 10 to 20 mmHg, stroke volume of WT hearts showed no more increase and a decrease at 20 mmHg. In contrast, cTnI-ND,*Tnni3*$^{-/-}$ hearts continued increasing of stroke volume, demonstrating extended Frank-Starling response (Fig. 1 B).

With the enhanced positive response of ventricular stroke volume to preload, the two primary parameters of Frank-Starling law, cTnI-ND,*Tnni3*$^{-/-}$ hearts maintained the left ventricular peak pressure (LVP_{max}; Fig. 2 A) and development pressure (LVP_{dev}; Fig. 2 B) at high preloads while WT hearts showed notable decreases. LV systolic velocity, $+dP/dt_{max}$, of cTnI-ND,*Tnni3*$^{-/-}$ hearts was slightly lower than WT controls at lower preloads of 3–10 mmHg, likely reflecting the effect of cTnI-ND on decreasing myofilament Ca^{2+} sensitivity (Barbato et al., 2005). At higher preloads, $+dP/dt_{max}$ of cTnI-ND,*Tnni3*$^{-/-}$ and WT hearts became similar and plateaued at preloads from 12.5 to 20 mmHg (Fig. 2 C).

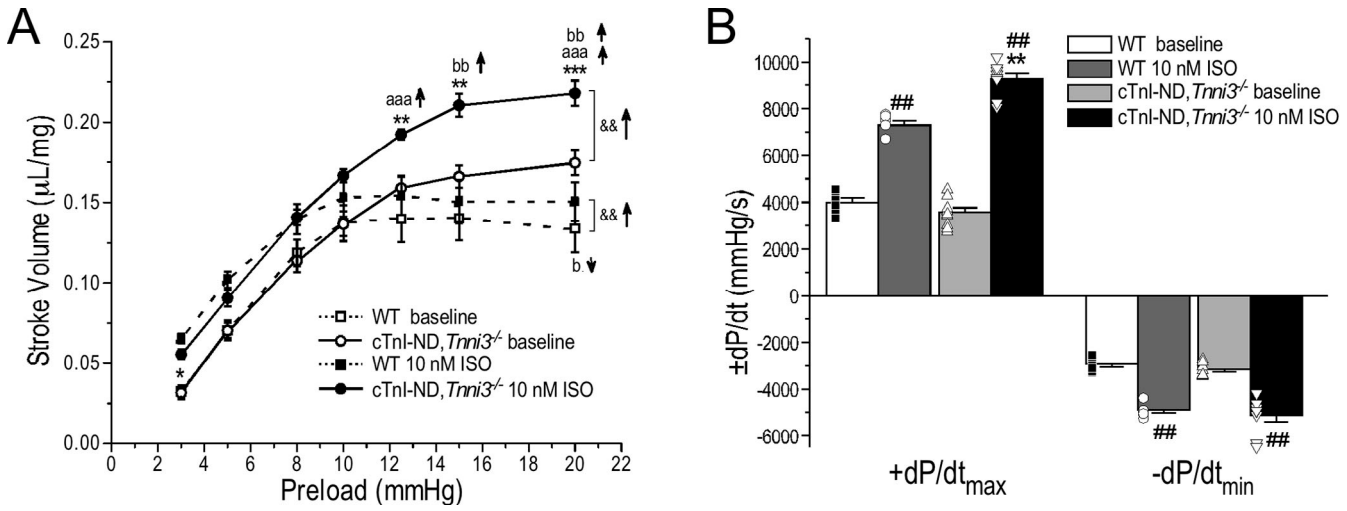

Figure 4. **The enhanced Frank-Starling response of cTnI-ND,*Tnni3*$^{-/-}$ hearts is augmented by β-adrenergic stimulation.** Functions of ex vivo working heart were measured in the absence (baseline) or presence of ISO. **(A)** The stroke volume curves show that 10 nM ISO augmented the Frank-Starling responses of WT hearts and had much higher effect on the already enhanced response of cTnI-ND,*Tnni3*$^{-/-}$ hearts at preload of 10–20 mmHg. **(B)** At 10 mmHg preload, 10 nM ISO produced a larger increase in contractile velocity (+dP/dt$_{max}$) in cTnI-ND,*Tnni3*$^{-/-}$ hearts than that in WT hearts, whereas the effects on increasing relaxation velocity (−dP/dt$_{min}$) were similar in the two groups. Values are mean ± SEM, n = 6 mice in WT and 9 mice in cTnI-ND,*Tnni3*$^{-/-}$ groups. $^{\&\&}P < 0.01$ vs. control in two-way ANOVA with post-hoc method of Tukey's test. $^{**}P < 0.01$ and $^{***}P < 0.001$ vs. WT in Student's t test. $^{aaa}P < 0.001$ vs. stroke volume at 10 mmHg preload; $^{b}P < 0.05$ and $^{bb}P < 0.01$ vs. 12.5 mmHg, and $^{\#\#}P < 0.01$ vs. baseline in paired Student's t test. ↑ and ↓ indicate increase and decrease in the comparisons.

In addition to LVP$_{max}$ and +dP/dt$_{max}$, LV ejection time (Fig. 3 A) also determines stroke volume (Feng et al., 2008a; Feng and Jin, 2010). LV ejection time increased in both cTnI-ND,*Tnni3*$^{-/-}$ and WT hearts when preload increased. Parallel with the changes in stroke volume (Fig. 1 B), LV ejection time plateaued in WT hearts when preload was raised above 12.5 mmHg whereas it continued increasing in cTnI-ND,*Tnni3*$^{-/-}$ hearts (Fig. 3 B). Dividing the LV ejection time into rapid and reduced phases (Fig. 3 A) revealed that the rapid ejection phase was similar in cTnI-ND,*Tnni3*$^{-/-}$ and WT hearts whereas the reduced ejection phase was significantly elongated in cTnI-ND,*Tnni3*$^{-/-}$ hearts at the higher preloads of 10–20 mmHg (Fig. 3 B), contributing to the longer total ejection time and the higher stroke volume (Fig. 1 B).

cTnI-ND,*Tnni3*$^{-/-}$ hearts preserved positive inotropic response to β-adrenergic stimulation with an enhanced response at higher preload

cTnI-ND,*Tnni3*$^{-/-}$ and WT ex vivo mouse working hearts were compared for response to physiological level of β-adrenergic stimulation with 10 nM ISO. The intrinsic sinus rate of the ex vivo mouse working hearts increased to above 480 bpm in both WT and cTnI-ND,*Tnni3*$^{-/-}$ groups so they were then paced at 540 bpm to produce constant rhythmic beats for functional measurements. ISO treatment increased stroke volume of both WT and cTnI-ND,*Tnni3*$^{-/-}$ hearts where cTnI-ND,*Tnni3*$^{-/-}$ hearts had significantly higher responses especially at preloads above 12.5 mmHg (Fig. 4 A). Measured at preload of 10 mmHg, ISO treatment produced significantly higher systolic and diastolic velocities in both groups while cTnI-ND,*Tnni3*$^{-/-}$ hearts showed higher systolic response (+dP/dt, Fig. 4 B). The results demonstrate that cTnI-ND,*Tnni3*$^{-/-}$ hearts have not only preserved but also enhanced the inotropic potential upon β-adrenergic stimulation to increase Ca^{2+} activation of myofilaments.

Phosphorylation of phospholamban by PKA is a potent mechanism to increase the activity of SERCA2a Ca^{2+} pump upon β-adrenergic stimulation to enhance cardiac muscle contractility (Bers et al., 2006). The Western blots and densitometry quantification in Fig. 5 A showed that the expression levels of SERCA2a in cTnI-ND,*Tnni3*$^{-/-}$ and WT control hearts are similar. The results in Fig. 5 B further show that the levels of total phospholamban protein were similar in cTnI-ND,*Tnni3*$^{-/-}$ and WT hearts and Ser^{16}-phosphorylated phospholamban increased similarly in both groups upon ISO treatment. These results suggest that the cytosolic Ca^{2+} handling was not altered in cTnI-ND,*Tnni3*$^{-/-}$ cardiomyocytes, and the deletion of PKA substrate Ser^{23}/Ser^{24} of cTnI by N-terminal truncation does not alter PKA phosphorylation of phospholamban and SERCA2a function, supporting the notion that cTnI-ND enhances Frank-Starling response through modulating myofilament functions.

Cardiac myosin binding protein C (cMBP-C) is another PKA substrate in cardiomyocyte (Hartzell and Glass, 1984) and a potential contributor to Frank-Starling response (Kumar et al., 2015). The Pro-Q stained SDS-gel in Fig. 6 A confirms that intact cTnI was phosphorylated at a significant level in WT mouse heart whereas the N-terminal truncated cTnI in cTnI-ND,*Tnni3*$^{-/-}$ mouse heart had no detectable phosphorylation due to the lack of Ser^{23}/Ser^{24}. Densitometry quantification showed that the deletion of Ser^{23}/Ser^{24} from cTnI did not change the level of ISO-stimulated phosphorylation of cMBP-C in cTnI-ND,*Tnni3*$^{-/-}$ hearts in vivo (Fig. 6 B). This observation was confirmed by Pro-Q staining and quantification of phosphoproteins in ISO-treated ex vivo cTnI-ND,*Tnni3*$^{-/-}$ and control WT working hearts (Fig. 6, C and D). The results demonstrate

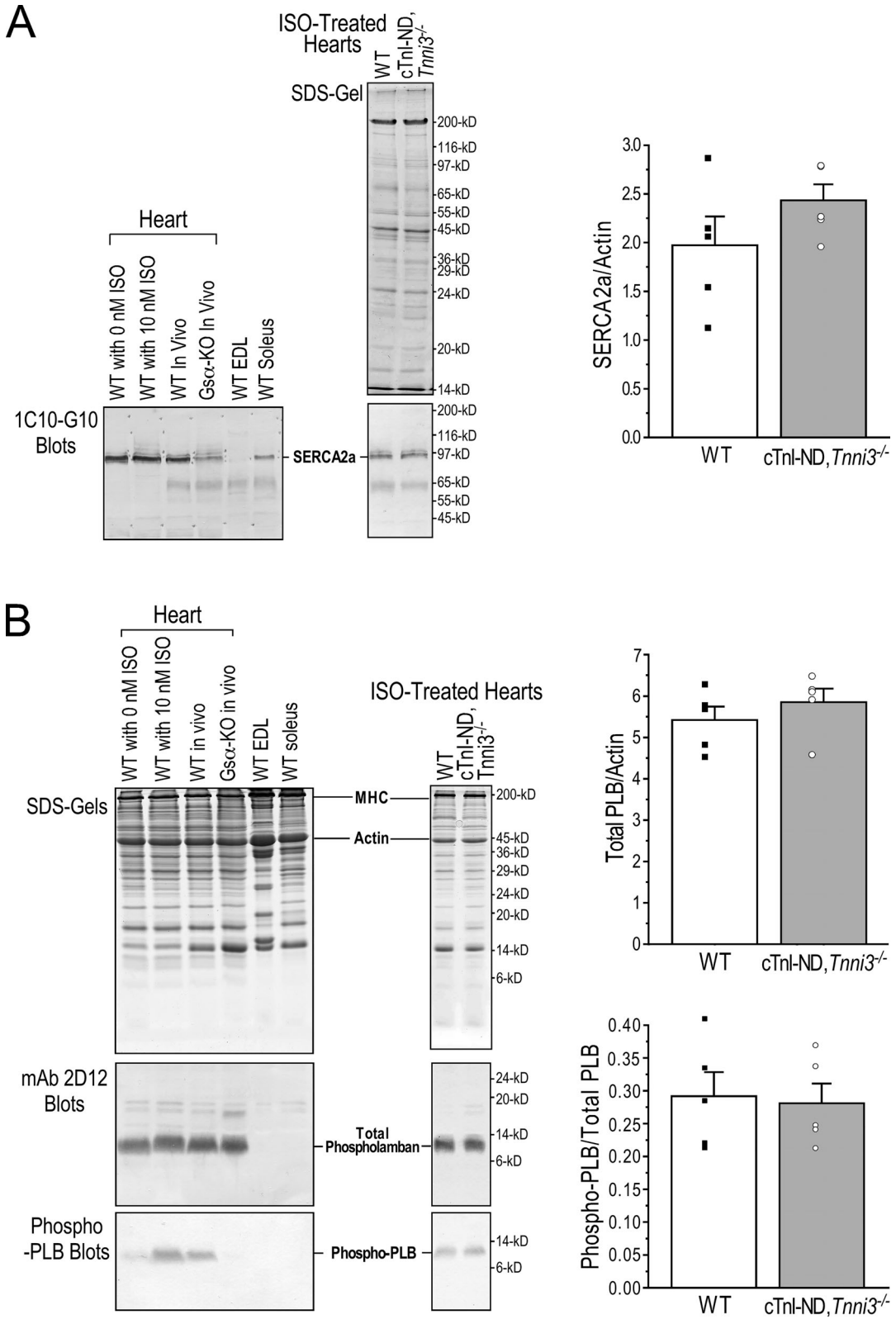

Figure 5. **Function of SERCA2a Ca^{2+} pump is unchanged in cTnI-ND,*Tnni3*$^{-/-}$ mouse hearts. (A)** The SDS-PAGE gel and Western blot show high level expression of SERCA2a in mouse heart and slow fiber-rich soleus muscle but not in fast fiber type extensor digitorum longus (EDL) muscle, which was decreased in the Gsα knockout (Gsα-KO) failing heart control (Feng et al., 2008b). Densitometry quantification normalized to actin showed that the levels of SERCA2a were not significantly different in cTnI-ND,*Tnni3*$^{-/-}$ and WT hearts. **(B)** The Western blots show the expected expression of phospholamban (PLB), a regulator of SERCA2a, in mouse heart but not in skeletal muscles and the increased phosphorylation of PLB when ex vivo mouse working hearts were treated with 10 nM ISO. β-adrenergic defective Gsα-KO mouse heart was used as a negative control. Densitometry quantification normalized to actin showed similar levels of total PLB expression and phosphorylation upon ISO treatment in cTnI-ND,*Tnni3*$^{-/-}$ and WT hearts. Values are mean ± SEM. $n = 5$ mice each in WT and cTnI-ND,*Tnni3*$^{-/-}$ groups. Statistical analysis was performed using Student's t test, and no significant difference was found. MHC, myosin heavy chain.

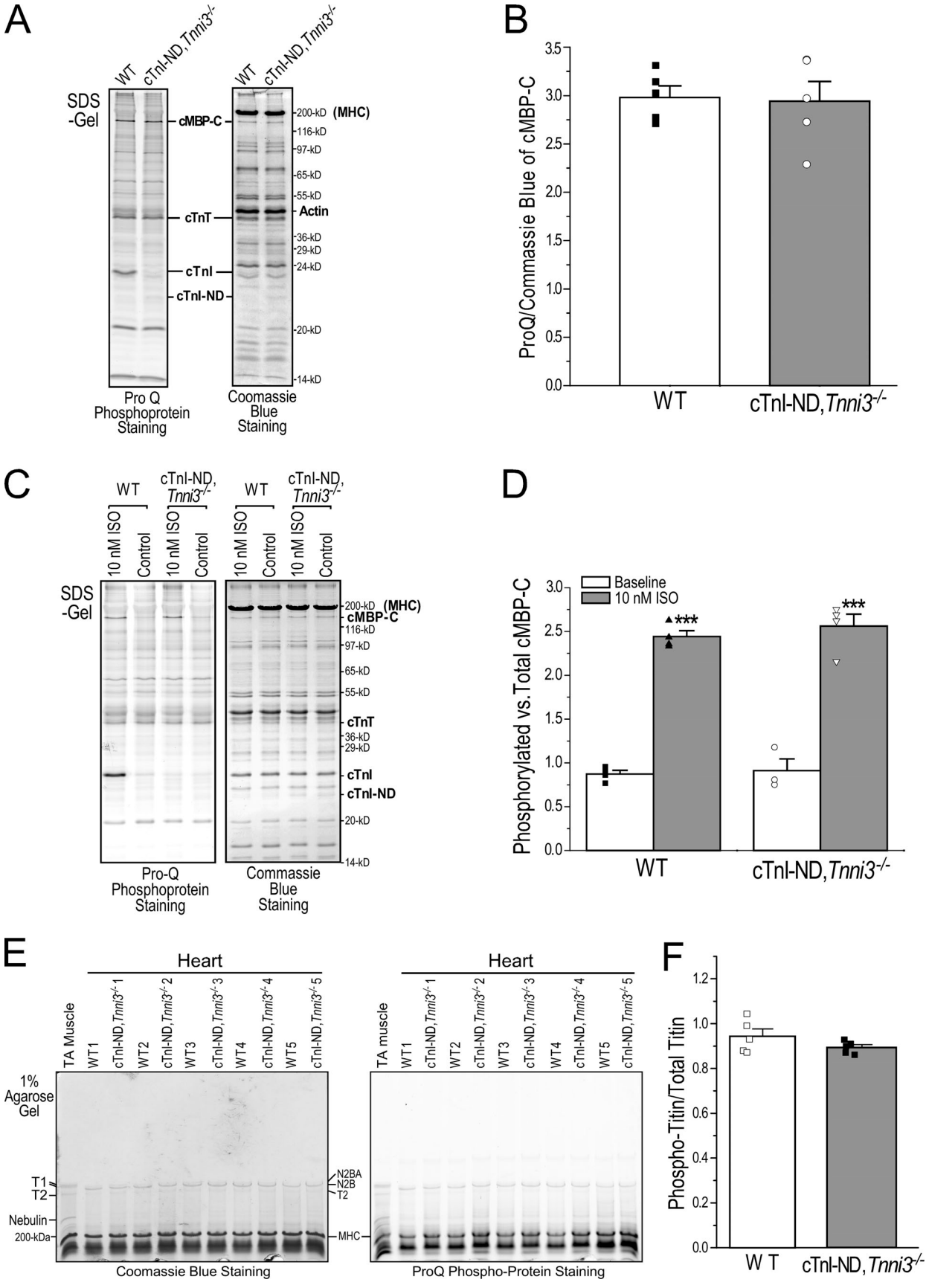

Figure 6. **The loss of N-terminal PKA phosphorylation sites in cTnI-ND,*Tnni3*$^{-/-}$ mouse heart does not alter PKA phosphorylation of cMBP-C and titin.** **(A)** The SDS-PAGE gel stained for phosphoprotein using Pro-Q reagent shows the significant phosphorylation of cMBP-C and intact cTnI in WT mouse hearts

treated with ISO in vivo. cTnI-ND in cTnI-ND,*Tnni3*$^{-/-}$ mouse hearts had no detectable phosphorylation, consistent with the fact that PKA phosphorylation of cTnI is primarily at the N-terminal Ser^{23}/Ser^{24}. **(B)** Densitometry quantification showed that the loss of a major PKA substrate in cTnI-ND,*Tnni3*$^{-/-}$ hearts did not alter the level of ISO-stimulated PKA phosphorylation of cMBP-C. **(C)** The Pro-Q phosphoprotein stained SDS-gel shows that the level of cMBP-C phosphorylation was increased in ex vivo working hearts upon 10 nM ISO treatment. **(D)** Densitometry quantification showed similar degrees of cMBP-C phosphorylation in cTnI-ND,*Tnni3*$^{-/-}$ and WT hearts at baseline and after ISO treatment. **(E and F)** The agarose SDS-gels stained for total proteins and phosphoproteins and densitometry quantification showed no difference in titin splice form or in the degrees of phosphorylation in cTnI-ND,*Tnni3*$^{-/-}$ and WT hearts. MHC, myosin heavy chain. Values are mean ± SEM. *n* = 3–5 mice in each group. ***P < 0.001 vs. baseline in Student's *t* test.

that the larger β-adrenergic effect on enhancing Frank-Starling response in cTnI-ND,*Tnni3*$^{-/-}$ hearts was not from altering the phosphorylation of cMBP-C.

Titin is also a substrate of PKA in cardiomyocytes to affect resting tension in HFpEF (LeWinter and Granzier, 2014). The SDS-agarose gel in Fig. 6 E shows that titin splice forms were not different in WT and cTnI-ND,*Tnni3*$^{-/-}$ mouse hearts. Phosphorylation of titin detected by Pro-Q diamond staining and densitometry quantification also showed no difference between WT and cTnI-ND,*Tnni3*$^{-/-}$ hearts (Fig. 6, E and F), indicating the functional changes in cTnI-ND,*Tnni3*$^{-/-}$ hearts was not based on titin modifications.

The enhanced Frank-Starling response of cTnI-ND,*Tnni3*$^{-/-}$ hearts was not based on increased LV end diastolic volume

In vivo cardiac function and β-adrenergic effect were studied using echocardiography. ISO treatment in vivo rapidly increased the heart rates of WT and cTnI-ND,*Tnni3*$^{-/-}$ mice from 481.8 ± 3.75 to 518 ± 2.77 and 482.6 ± 4.35 to 514.0 ± 8.48 bpm, respectively, indicating similar degrees of systemic β-adrenergic response (Table 2). The results showed that ISO treatment reduced left ventricular end diastolic dimension (LVEDD) similarly in WT and cTnI-ND,*Tnni3*$^{-/-}$ mice but produced significantly more increases of systolic function in cTnI-ND,*Tnni3*$^{-/-}$ hearts as shown by the smaller left ventricular end systolic dimension (LVESD), higher fractional shortening and higher ejection fraction.

Ex vivo working heart studies further demonstrated that the left ventricular end diastolic volume (LVEDV) was similar in cTnI-ND,*Tnni3*$^{-/-}$ and WT control hearts. The representative LV P-V loops in Fig. 7 A show higher stroke volume of cTnI-ND,*Tnni3*$^{-/-}$ hearts at preload of 20 mmHg in comparison with that of WT hearts whereas their LVEDV were not different at the wide range of preloads tested (Fig. 7 B). cTnI-ND,*Tnni3*$^{-/-}$ hearts also showed a flatter LV end diastolic pressure-volume relationship (EDPVR) in comparison with that of WT hearts (Fig. 7 A).

cTnI-ND,*Tnni3*$^{-/-}$ and WT mouse cardiac muscles have similar optimal resting SLs

Histology study showed that the SL in LV papillary muscle fixed at optimal length for producing maximal active force was similar in cTnI-ND,*Tnni3*$^{-/-}$ and WT hearts (Fig. 8 A), supporting the observation that cTnI-ND can enhance Frank-Starling response without increasing LV diastolic dimension and volume.

Isolated cardiomyocytes from adult cTnI-ND,*Tnni3*$^{-/-}$ and WT mice showed similar slack resting SL in the presence of 10 mM BDM and absence of external load (Fig. 8 B), precluding notable structural remodeling at the sarcomere level, further supporting cTnI-ND's effect on enhancing Frank-Starling response by increasing the activation of myofilament in response to resting tension.

cTnI-ND enhances Frank-Starling response with decreased LVEDP

Consistent with the previous finding that the restrictive deletion of the N-terminal extension of cTnI mimics the effect of PKA phosphorylation of the N-terminal extension at Ser^{23}/Ser^{24} to decrease myofilament Ca^{2+} affinity and increases relaxation velocity (Barbato et al., 2005), cTnI-ND,*Tnni3*$^{-/-}$ hearts showed

Table 2. **In vivo echocardiograph of cTnI-ND,*Tnni3*$^{-/-}$ and WT mice and the effect of ISO treatment**

	WT (*n* = 5)			cTnI-ND,Tnni3$^{-/-}$ (*n* = 5)		
	Baseline	ISO treated	Δ difference	Baseline	ISO treated	Δ difference
Body weight (g)	17.54 ± 0.36			17.07 ± 0.21		
Heart rate (bpm)	481.8 ± 3.75	518.4 ± 2.77	+36.6 ± 5.12	482.6 ± 4.35	514 ± 8.48	+31.4 ± 7.32
LVEDD (mm)	2.89 ± 0.11	2.65 ± 0.07	−0.23 ± 0.06	3.04 ± 0.08	2.78 ± 0.10	−0.26 ± 0.06
LVESD (mm)	1.44 ± 0.06	1.162 ± 0.06	−0.28 ± 0.08	1.58 ± 0.12	1.04 ± 0.12	−0.55 ± 0.03*
Fractional shortening %	50.51 ± 1.24	57.55 ± 2.08	+7.04 ± 1.80	48.07 ± 2.88	62.87 ± 3.53	+14.8 ± 1.39*
Ejection fraction %	83.09 ± 1.08	88.45 ± 1.51	+5.36 ± 1.50	80.24 ± 3.132	91.53 ± 2.22	+11.29 ± 1.29*

In vivo cardiac functions were measured using echocardiography in 2-mo-old female WT and cTnI-ND,*Tnni3*$^{-/-}$ double transgenic mice. The ISO treatment (0.2 mg/kg) was given by i.p. injection. The functional parameters showed changes after ISO treatment as compared with the baseline in both WT and cTnI-ND,*Tnni3*$^{-/-}$ groups, in which paired Student's *t* test showed significantly larger responses in LVESD, fraction shortening, and ejection fraction (*P < 0.05 vs. WT control). The values shown are mean ± SEM. *n* = 5 mice in each group.

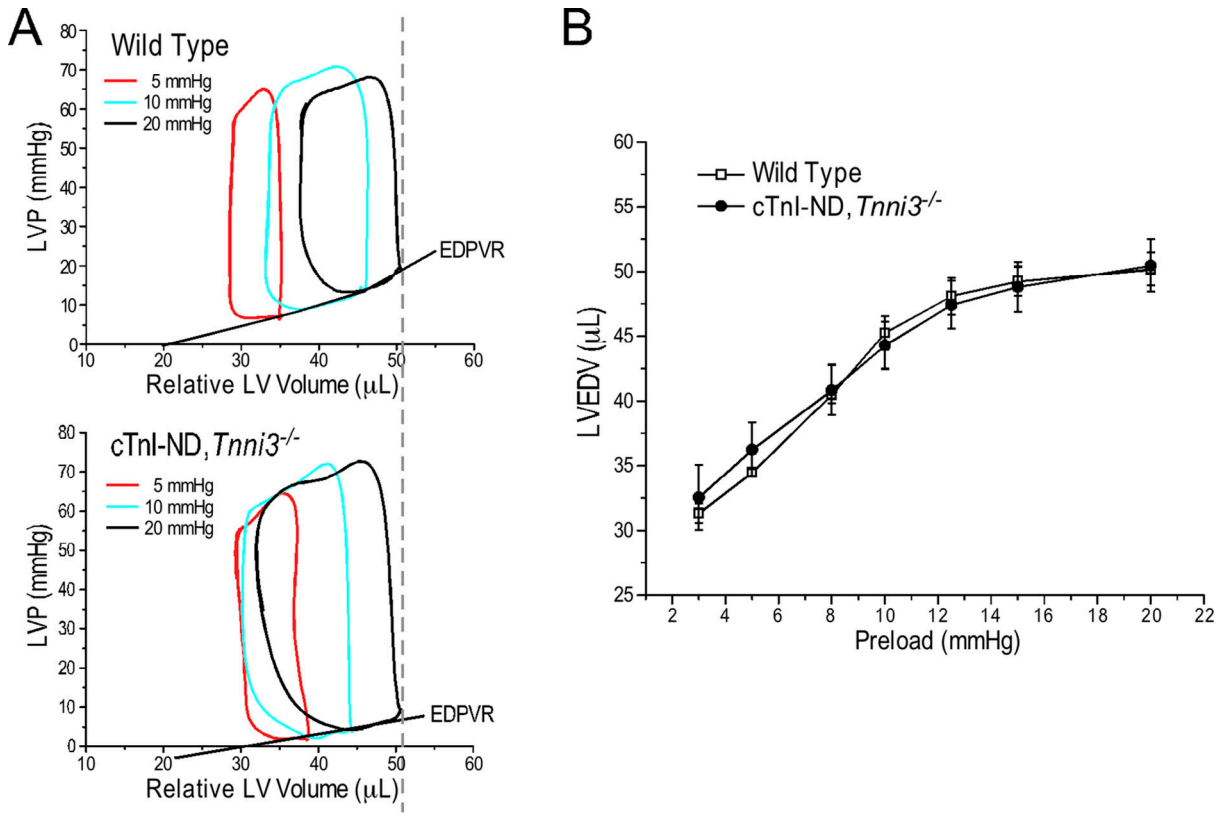

Figure 7. **cTnI-ND,*Tnni3*$^{-/-}$ hearts showed unchanged LVEDV but flatter LV EDPVR in comparison with that of WT hearts. (A)** The representative LV P-V loops of ex vivo working hearts at 5, 10, and 20 mmHg preloads illustrate the larger fraction shortening/stroke volume of cTnI-ND,*Tnni3*$^{-/-}$ hearts than that of WT hearts at high preloads while their LVEDV are similar. The slope of LV EDPVR of cTnI-ND,*Tnni3*$^{-/-}$ hearts is flatter than that of WT hearts, consistent with enhanced myocardial relaxation that increases ventricular diastolic compliance. **(B)** The quantitative data confirmed similar LVEDV of cTnI-ND,*Tnni3*$^{-/-}$ and WT hearts at various preloads. The values are mean ± SEM. *n* = 5–6 mice in WT and 8–9 mice in cTnI-ND,*Tnni3*$^{-/-}$ groups. Statistical analysis was performed using two-way ANOVA with post-hoc method of Tukey's test, and no significant difference was found.

higher ventricular relaxation velocity ($-dP/dt_{min}$; Fig. 9 A) and lower left ventricular end diastolic pressure (LVEDP; Fig. 9 B) than that of WT hearts at the higher preloads of 10–20 mmHg. With enhanced diastolic function, cTnI-ND,*Tnni3*$^{-/-}$ hearts exhibit lower LVEDP than that of WT hearts at a given LVDEV (Fig. 9 C), corresponding to a flatter LV EDPVR (Fig. 9 D). The results indicate that cTnI-ND enhances Frank-Starling response of cardiac muscle without increasing diastolic resting tension.

cTnI-ND enhances Ca^{2+} sensitivity response of activated skinned papillary muscle to SL

Using cryosection-derived skinned LV papillary muscle strips (Feng and Jin, 2020) that provide uniform cross-sectional area and precisely measurable sarcomeric striations (Fig. 10 A) for reliable quantitative measurements of length–tension and passive tension–active tension relationships, the force–pCa curves of WT and cTnI-ND,*Tnni3*$^{-/-}$ mouse cardiac muscle in Fig. 10 B show left shifts when SL was increased from 2.0 to 2.15 μm and to 2.3 μm in both groups (the slack SL lengths were 1.83–1.90 μm). cTnI-ND,*Tnni3*$^{-/-}$ cardiac muscle however had significantly higher increases in Ca^{2+} sensitivity in response to increases in SL than that of WT control. This functional effect of cTnI-ND is more potent in the activated state at higher [Ca^{2+}], resulting a trend of increase in cooperativity of Ca^{2+} activation of force production (Fig. 10 B, inset table).

The mechanical studies showed expected SL dependent increases of resting and activated tensions (Fig. 10, C and D, respectively) similar to literature data from traditional skinned muscle studies. [Ca^{2+}] for developing 50% maximum force (pCa50) indicated that cTnI-ND,*Tnni3*$^{-/-}$ cardiac muscle had a trend of higher Ca^{2+} sensitivity at longer SL than WT control (Fig. 10 E), which was statistically significant when comparing pCa90 as an index to the activated state (Fig. 10 F).

cTnI-ND increases myofilament Ca^{2+} sensitivity in response to resting passive tension

While plotting the pCa90 of skinned cardiac muscle strips as a function of SL revealed a steeper slope in cTnI-ND,*Tnni3*$^{-/-}$ than that of WT group (Fig. 11 A), plotting the resting passive tension against SL showed nearly identical slops for the two groups precluding a direct length effect (Fig. 11 B). An informative finding is that plotting pCa90 as a function of the cross sectional area-normalized resting passive tension produced a steeper slope for cTnI-ND,*Tnni3*$^{-/-}$ cardiac muscle strips than WT control (Fig. 11 C). The results demonstrate that cTnI-ND enhances

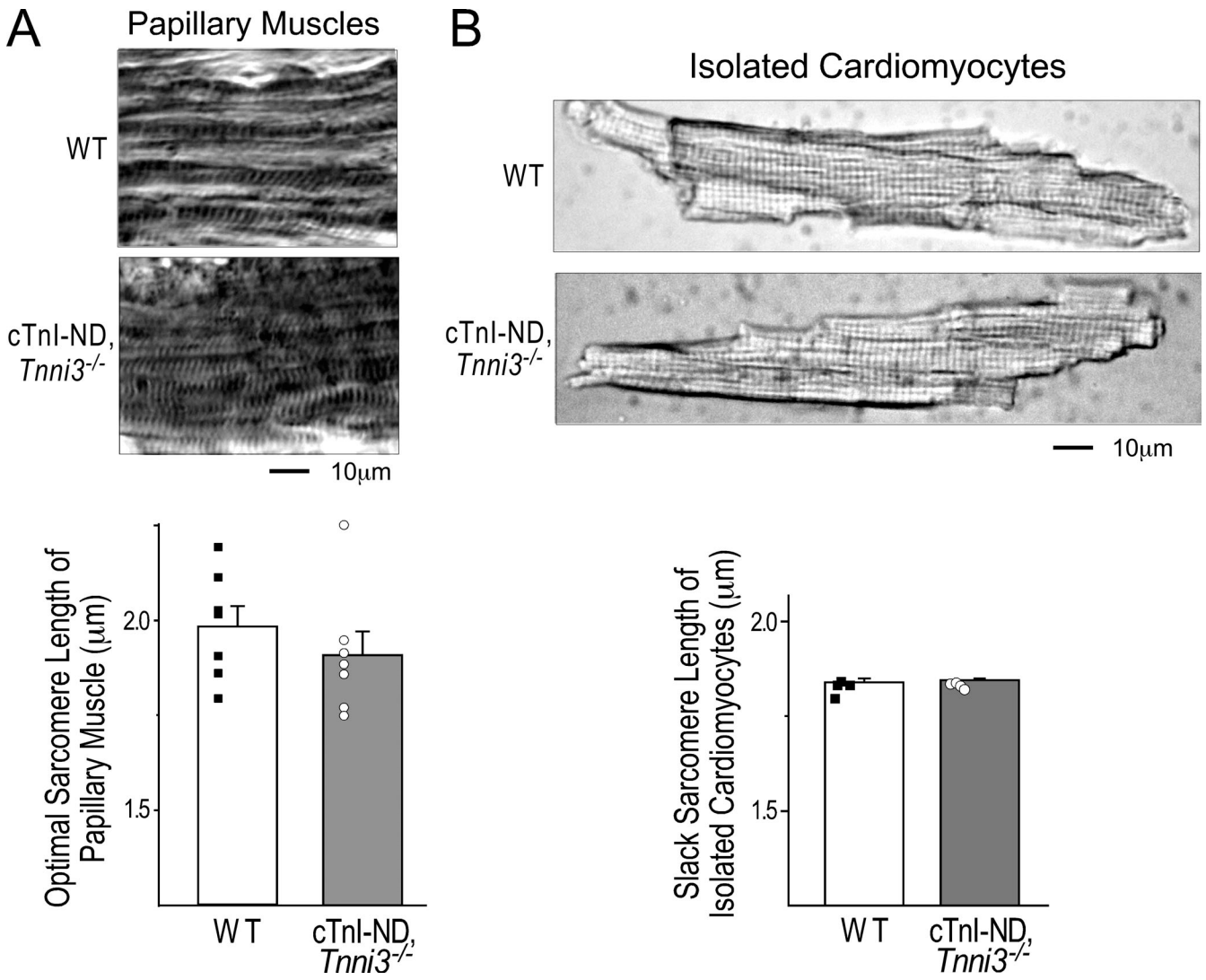

Figure 8. **cTnI-ND does not alter the optimal resting SL in papillary muscles and the slack SL in isolated cardiomyocytes. (A)** The longitudinal sections of LV papillary muscle fixed at the length of maximum force development and quantitative measurements showed that cTnI-ND,*Tnni3*$^{-/-}$ and WT cardiac muscles have similar optimal resting SL. **(B)** The representative micrographs and quantitative analysis show that cardiomyocytes isolated from adult cTnI-ND,*Tnni3*$^{-/-}$ and WT mouse hearts have similar SL in the presence of 10 mM BDM and absence of external load. 25–30 cells were measured from each heart. Values are mean ± SEM. *n* = 4–7 mice each in WT and cTnI-ND,*Tnni3*$^{-/-}$ groups. Statistical analysis was done using Student's *t* test, and no significant difference was found.

Frank-Starling response of cardiac muscle through producing a higher response to resting tension, rather than directly based on increase in SL, to increase myofilament Ca^{2+} sensitivity.

Discussion

The N-terminal extension of cTnI is an evolutionarily added regulatory structure specific to postnatal heart of higher vertebrates (Sheng and Jin, 2016; Rasmussen et al., 2022). This structure is posttranslationally modified by PKA phosphorylation at Ser^{23}/Ser^{24} or restrictive proteolytic truncation to modulate the conformation and function of cTnI (Akhter et al., 2012) and myocardial contractility (McConnell et al., 1998; Kentish et al., 2001; Yu et al., 2001; Layland et al., 2005; Feng et al., 2008b). The present study investigated the effect of cTnI-ND on Frank-Starling response of the heart. The results provide several novel insights into the underlying mechanisms.

N-terminal-truncated cTnI enhances Frank-Starling response of the heart

cTnI-ND was first discovered as an adaptation to decreased cardiac function in simulated chronic microgravity (Yu et al., 2001). This compensatory adaptation also occurs in β-adrenergic deficient failing hearts of Gsα KO mice (Feng et al., 2008b) and mice with deficiency of A-kinase anchoring protein (McConnell et al., 2009). Previous transgenic mouse model with overexpression of cTnI-ND partially respace the endogenous intact cTnI at 70–80% showed enhanced diastolic function (Barbato et al., 2005; Feng et al., 2008b), implicating a role of cTnI-ND

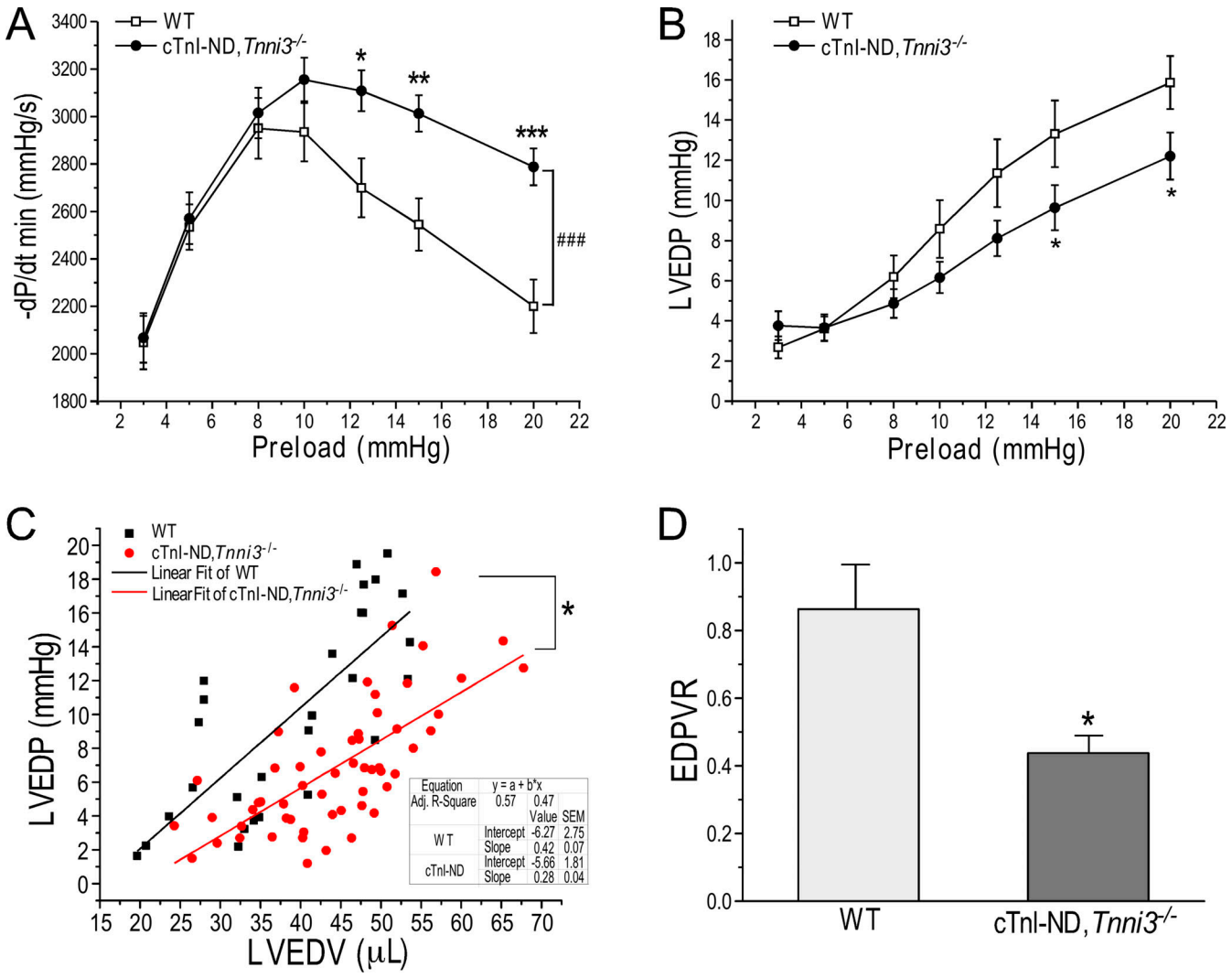

Figure 9. **cTnI-ND enhances LV relaxation. (A)** cTnI-ND,*Tnni3*$^{-/-}$ and WT mouse hearts showed similar relaxation velocities (–dP/dt$_{min}$) and increases when preload increased from 3 to 8 mmHg. At higher preloads of 12.5–20 mmHg, LV –dP/dt$_{min}$ decreases which was significantly less in cTnI-ND,*Tnni3*$^{-/-}$ hearts than WT control, rendering significantly higher LV relaxation velocity of cTnI-ND,*Tnni3*$^{-/-}$ hearts. **(B)** Consistently, the increase in LVEDP due to increase of preload was significantly less in cTnI-ND,*Tnni3*$^{-/-}$ hearts than that in WT hearts. Values are mean ± SEM. *n* = 6 mice in WT and 9 mice in cTnI-ND,*Tnni3*$^{-/-}$ groups for data in A and B. *P < 0.05, **P < 0.01, and ***P < 0.001 vs. WT in Student's *t* test; #P < 0.05 and ###P < 0.001 vs. WT in two-way ANOVA with post-hoc method of Tukey's test. **(C and D)** Data from the LVEDV and LVEDP of P-V loops were fitted with linear correlation to demonstrate the significantly different slopes of WT and cTnI-ND,*Tnni3*$^{-/-}$ groups for the effect of cTnI-ND on LVEDP volume relationship (LVEDVR, calculated using the average slopes values; D). *n* = 4 for WT and 8 for cTnI-ND,*Tnni3*$^{-/-}$ groups for data in C and D. *P < 0.05 vs WT in Student's *t* test.

in Frank-Starling response. To test this hypothesis avoiding the coexistence of intact cTnI, the present study used cTnI-ND,*Tnni3*$^{-/-}$ double transgenic mice expressing solely cTnI-ND in the cardiac muscle (Fig. 1 A). Ex vivo working hearts with precisely controlled preload and accurately measured stroke volume clearly demonstrated that cTnI-ND produces an augmented increase of stroke volume in response to increase of preload in comparison with the WT control (Fig. 1 B).

The enhanced Frank-Starling response of cTnI-ND,*Tnni3*$^{-/-}$ hearts is based on increased inotropic functions shown by the higher maximum LV pressure development and systolic velocity (Fig. 2). cTnI-ND elongates the reduced ejection phase (Fig. 3 B) corresponding to the beginning of diastole of the ventricle, which may indicate an effect of cTnI-ND on increasing myofilament Ca^{2+} sensitivity more potently in the activated state at the end of systole (as reflected by the effect on pCa90 shown in Fig. 10 B). The possible effect of cTnI-ND on the number of active cross bridges (Smith et al., 2009) merits further investigation. It is worth noting that the effect of cTnI-ND on enhancing Frank-Starling response is more predominant at preloads higher than 10 mmHg, above the normal LVEDP of mouse in vivo. This could be beneficial in compensating cardiac function in congestive heart failure where LVEDP/preload increases. Supporting this notion, adaptive increases of cTnI-ND were found in heart failure conditions as a compensatory response (Yu et al., 2001; Feng et al., 2008b).

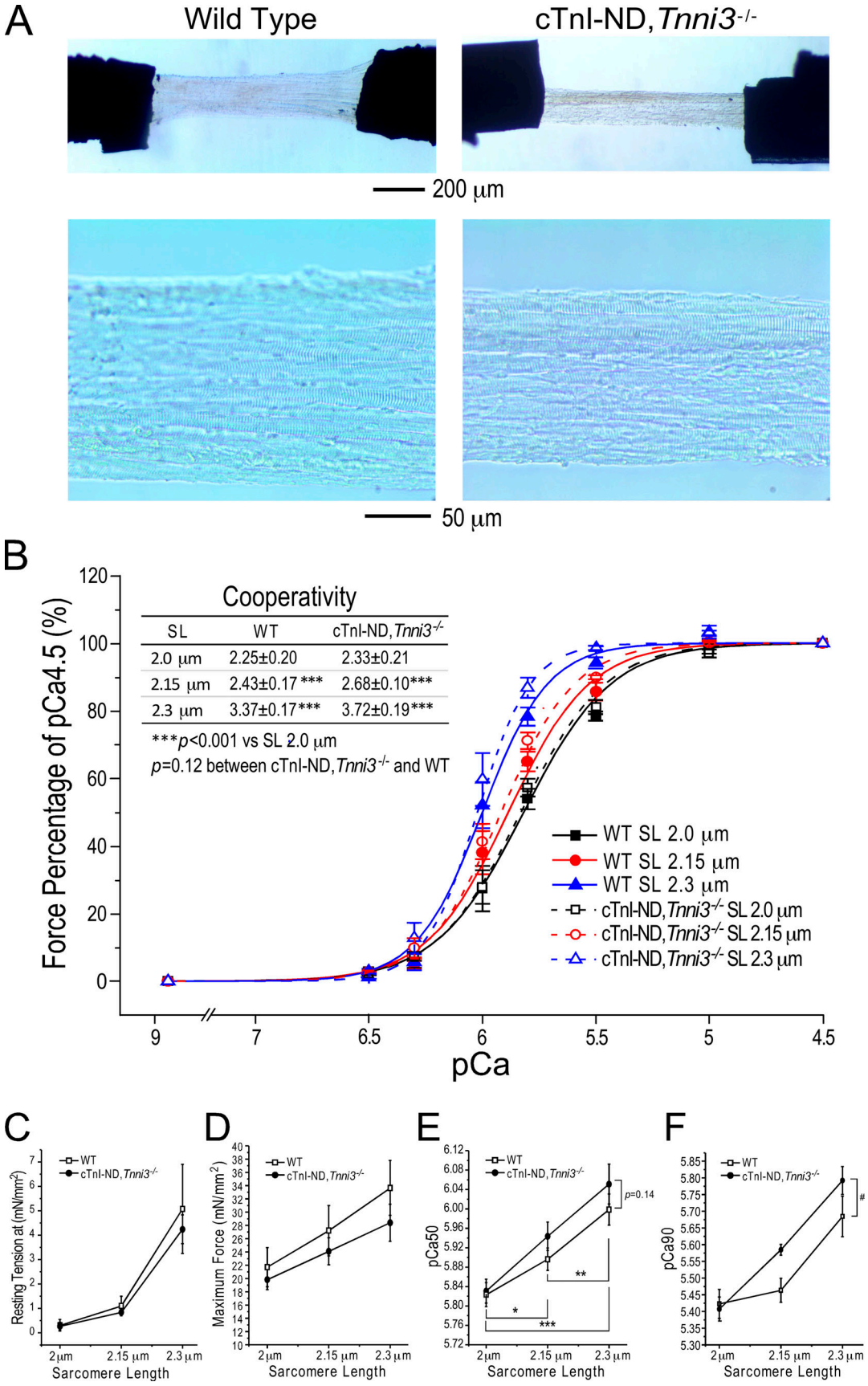

Figure 10. **cTnI-ND increases the SL-dependent increase of myofilament Ca^{2+} sensitivity. (A)** Cryosection-derived detergent skinned LV papillary muscle strips mounted between force transducer and length lever arm provide uniform thin preparations with clear striations under light microscope for an accurate

determination of SL in contractility studies. **(B)** Isometric force–pCa curves of skinned papillary muscle sections normalized to maximum force at pCa 4.5 showed left shifts in WT and cTnI-ND,*Tnni3*$^{-/-}$ groups when SL was increased from 2.0 to 2.15 and to 2.3 µm. cTnI-ND,*Tnni3*$^{-/-}$ muscle showed higher increases in Ca^{2+} sensitivity than WT control at SL of 2.15 and 2.3 µm. The effect of cTnI-ND is larger at higher [Ca^{2+}], resulting in a trend of increase in the cooperativity of myofilament activation (the inset table). **(C and D)** Resting tension at pCa 9 (C) and maximum active force developed at pCa 4.5 (D) did not show significant difference between cTnI-ND,*Tnni3*$^{-/-}$ and WT groups (the trends of lower passive tension and higher active tension in cTnI-ND,*Tnni3*$^{-/-}$ muscle strips at longer SL did not reach statistical significance). **(E)** The pCa50 values demonstrate the anticipated higher Ca^{2+} sensitivity at longer SL in both cTnI-ND,*Tnni3*$^{-/-}$ and WT muscle strips, in which cTnI-ND,*Tnni3*$^{-/-}$ group showed a trend of greater response. **(F)** The differences became statistically significant when pCa90 was compared, indicating a mechanism that is more effective on activated myofilaments. Values are mean ± SEM. n = 5 strips from three mice each in cTnI-ND,*Tnni3*$^{-/-}$ and WT groups. *P < 0.05, **P < 0.01, ***P < 0.001 vs. WT in paired Student's t test, and #P < 0.05 vs. SL at 2.0 or 2.15 µm in two-way ANOVA with post-hoc method of Tukey's test.

cTnI-ND,*Tnni3*$^{-/-}$ cardiac muscle retains the response to β-adrenergic stimulation with augmented Frank-Starling response

The physiological concentration of ISO (10 nM) increased Frank-Starling response in both WT and cTnI-ND,*Tnni3*$^{-/-}$ mouse ex vivo working hearts while cTnI-ND,*Tnni3*$^{-/-}$ hearts showed a significantly higher response (Fig. 4) suggesting enhanced myofilament response to Ca^{2+} activation. This was also seen in vivo in echocardiography as increased LV ejection fraction in ISO-treated cTnI-ND,*Tnni3*$^{-/-}$ mice (Table 2). cTnI-ND,*Tnni3*$^{-/-}$ and control WT hearts showed no difference in the expression of SERCA2a pump and the phosphorylation of phospholamban (Fig. 5). Therefore, the higher β-adrenergic response of cTnI-ND,*Tnni3*$^{-/-}$ hearts with enhanced Frank-Starling response is attributed to increased myofilament response to Ca^{2+} since a previous study showed similar intracellular Ca^{2+} transients in cTnI-ND,*Tnni3*$^{-/-}$ and WT cardiomyocytes while cTnI-ND cells produced higher contractile amplitude and faster shortening and relengthening velocities (Wei and Jin, 2015).

β-adrenergic dependent PKA phosphorylation of cTnI at Ser^{23}/Ser^{24} in the N-terminal extension is known to increase Frank-Starling response (Hanft et al., 2013). Our previous study showed that PKA phosphorylation of Ser^{23}/Ser^{24} and deletion of the N-terminal extension produce similar and non-additive effects on the function of cTnI through similar conformational modulations to alter interactions with TnT and troponin C (TnC; Akhter et al., 2012; Akhter and Jin, 2015). Therefore, restrictive removal or PKA phosphorylation of the N-terminal extension of cTnI may function by the same downstream mechanism. The preserved response of cTnI-ND,*Tnni3*$^{-/-}$ hearts to β-adrenergic stimulation (Fig. 4) indicates that deletion of the N-terminal extension of cTnI selectively utilizes a downstream mechanism of β-adrenergic signaling to compensate for cardiac function without broad side effects. The half-life of troponin proteins in mammalian cardiac muscle is only 3–4 d (Martin, 1981). Therefore, cTnI-ND produced in physiological adaptations will be replaced by newly synthesized intact cTnI in a week, implicating a reversable therapeutic approach that merits more investigations.

cTnI-ND increases systolic function in response to preload without increasing LVEDV

The Frank-Starling law first described over a century ago stated a relationship between ventricular filling volume and pump function of the heart as a beat-to-beat response to adjust stroke volume. While the faster relaxation velocity in cTnI-ND,*Tnni3*$^{-/-}$ hearts facilitates ventricular filling, cTnI-ND,*Tnni3*$^{-/-}$ and WT hearts do not show differences in LVEDD in vivo (Table 2) or LVEDV in ex vivo working hearts (Fig. 7). The effect of cTnI-ND on enhancing Frank-Starling response without increasing end diastolic length of the cardiac muscle is further supported by unchanged optimal resting SL length in the production of maximum active force (Fig. 8 A).

Studies on the mechanisms of Frank-Starling response of cardiac muscles have been concentrated on the length-dependency of myofilament Ca^{2+} sensitivity (Allen and Kurihara, 1982; Shiels et al., 2006; Shiels and White, 2008; de Tombe et al., 2010). Our finding that cTnI-ND,*Tnni3*$^{-/-}$ enhances Frank-Starling response to preload without increasing LVEDV or resting SL opens a new dimension for mechanistic investigations. Previous studies have shown that PKA phosphorylation of cMBP-C plays a role in Frank-Starling response (Hanft et al., 2013; Kumar et al., 2015; Mamidi et al., 2016). The effect of phosphorylation of cMBP-C on cross-bridges may contribute to passive tension of cardiac muscle in the early phase of diastole, providing a SL independent mechanism to decrease tension and facilitate ventricular filling (Rosas et al., 2015). However, cTnI-ND,*Tnni3*$^{-/-}$ and WT hearts are not different in cMBP-C phosphorylation before and after ISO treatment (Fig. 6, C and D).

Cardiac titin plays an important role in passive properties and Frank-Starling response of cardiac muscle (Fukuda and Granzier, 2005). cTnI-ND,*Tnni3*$^{-/-}$ hearts however showed no difference in titin expression and PKA phosphorylation from that of WT hearts (Fig. 6, E and F).

cTnI-ND enhances Frank-Starling response by increasing myofilament sensitivity to passive tension

cTnI-ND,*Tnni3*$^{-/-}$ hearts exhibit faster $-dP/dt_{min}$ and lower LVEDP than WT controls especially at higher preload (Fig. 9, A and B). With unchanged LVEDV (Fig. 7 B), cTnI-ND,*Tnni3*$^{-/-}$ hearts show flatter EDPVR than that of WT hearts (Fig. 9. C and D). The data demonstrate that cTnI-ND enhances Frank-Starling response without increasing passive tension in the ventricular muscle. A previous study also observed this property (Cazorla et al., 2000) and suggested a myofilament-based hypothesis that increased number of cross-bridges at the weakly bound state may increase Ca^{2+} sensitivity at longer SL (de Tombe et al., 2010). Supporting the effect of cTnI-ND on facilitating cardiac muscle relaxation through modulating cross bridge kinetics, a previous stopped-flow spectrofluorimetry study showed that the ATP binding rate of isolated cardiac myofibrils from cTnI-ND mice is threefold faster than that of WT control at low Ca^{2+}

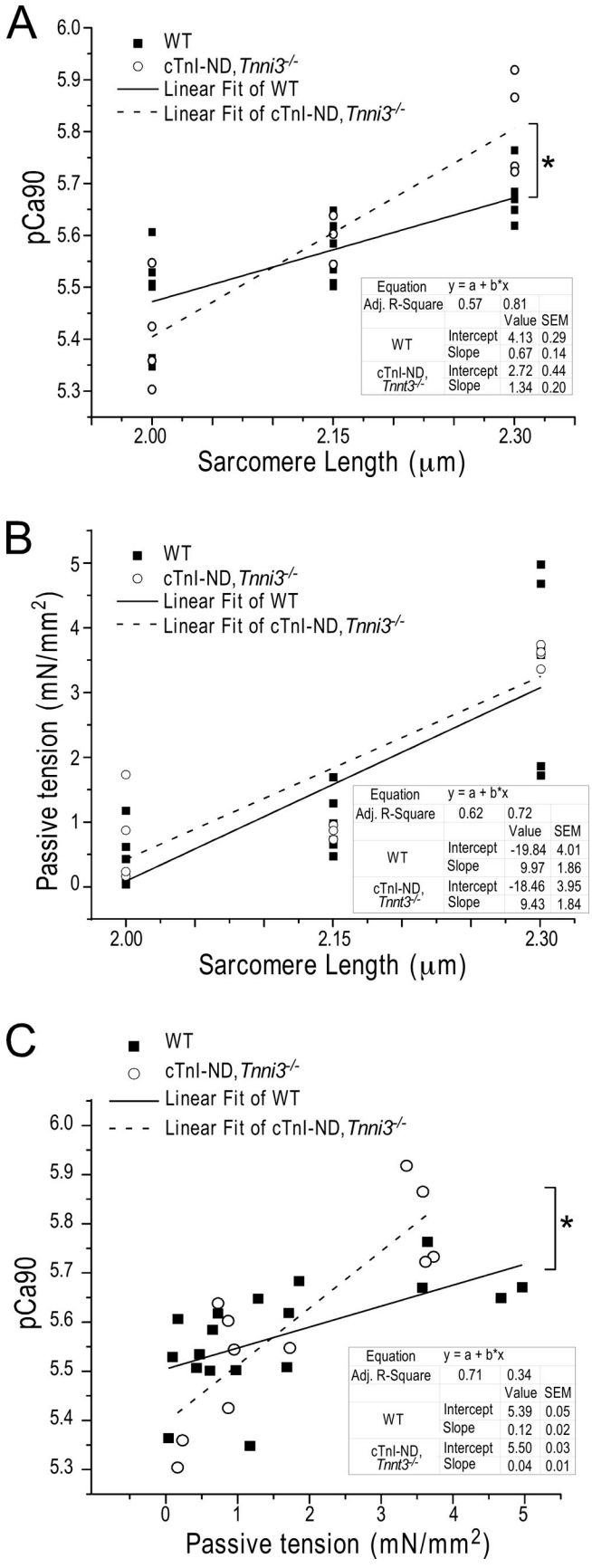

Figure 11. **cTnI-ND increases the response of myofilament Ca^{2+} sensitivity to passive tension other than SL.** The uniform cross-sectional area of cryosection-derived mouse papillary muscle strips empowers a reliable measurement of resting tension and compare between cTnI-ND,*Tnni3*$^{-/-}$ and WT cardiac muscles with precisely controlled SL. **(A)** Plotting pCa90 as a function of SL demonstrated a classic length dependent increase of Ca^{2+} sensitivity, in which cTnI-ND,*Tnni3*$^{-/-}$ muscle showed a greater response. **(B)** Plotting resting tension against SL found no difference between the two groups. **(C)** However, plotting pCa90 against resting tension reproduced the higher response of cTnI-ND,*Tnni3*$^{-/-}$ muscle than that of WT control. Values are mean ± SEM. Each dot represents one muscle strip. n = 5 mice with six strips for WT and 4 mice with four strips for cTnI-ND,*Tnni3*$^{-/-}$ groups. *P < 0.05 vs. WT in Student's t test.

(Gunther et al., 2016). A hypothesis is that the passive tension applied to the myofilaments transmits into protein conformational changes in which cTnI-ND may increase the response of the thin filament regulatory system to increase Ca^{2+} sensitivity in the development of active force without increasing SL.

Supporting this hypothesis, cTnI-ND,*Tnni3*$^{-/-}$ cardiac muscle showed a steeper response of Ca^{2+}-sensitivity (Fig. 11 A) but similar slopes of passive tension response (Fig. 11 B) to SL in comparison with WT controls. Therefore, the effect of cTnI-ND on increasing Ca^{2+}-sensitivity of cardiac myofilaments in Frank-Starling response is based on increasing the sensitivity to passive tension (Fig. 11 C). While the Frank-Starling law is traditionally viewed as a muscle length-tension relationship, our data demonstrate that passive tension applied to the myofilaments by hemodynamic parameters including the increase in resting muscle length is a determining mechanism of Frank-Starling response. In this mechanism, cTnI-ND increases the myofilament sensitivity to passive tension to enhance Frank-Starling response without increasing LVEDV (Fig. 7 and Table 2), optimal SL (Fig. 8 A), or LVEDP (Fig. 9 B). By functioning in the passive tension–active tension relationship to increase myofilament sensitivity and response to passive tension, cTnI-ND represents a physiological approach to producing greater force and improving the function of failing heart without increasing diastolic SL, which is particularly valuable for treating HFpEF where diastolic function is impaired to limit the lengthening of sarcomeres (Borlaug and Kass, 2006).

Acknowledgments

Henk L. Granzier served as editor.

We thank Ms. Hui Wang for technical assistance and Dr. Steven Cala for the 1C10G10 and 2D12 antibodies.

This study was supported by grants from the National Institutes of Health (HL127691 and HL138007) to J.-P. Jin.

The authors declare no competing financial interests.

Author contributions: H.-Z. Feng and J.-P. Jin conceived and designed the study. H.-Z. Feng and X. Huang performed the experiments. H.-Z. Feng, X. Huang and J.-P. Jin performed data analysis and interpreted data. H.-Z. Feng and J.-P. Jin drafted and revised the manuscript.

Submitted: 11 November 2020
Revised: 9 December 2022
Accepted: 29 December 2022

References

Akhter, S., and J.P. Jin. 2015. Distinct conformational and functional effects of two adjacent pathogenic mutations in cardiac troponin I at the interface with troponin T. *FEBS Open Bio.* 5:64–75. https://doi.org/10.1016/j.fob.2015.01.001

Akhter, S., Z. Zhang, and J.P. Jin. 2012. The heart-specific NH2-terminal extension regulates the molecular conformation and function of cardiac troponin I. *Am. J. Physiol. Heart Circ. Physiol.* 302:H923–H933. https://doi.org/10.1152/ajpheart.00637.2011

Allen, D.G., and S. Kurihara. 1982. The effects of muscle length on intracellular calcium transients in mammalian cardiac muscle. *J. Physiol.* 327: 79–94. https://doi.org/10.1113/jphysiol.1982.sp014221

Barbato, J.C., Q.Q. Huang, M.M. Hossain, M. Bond, and J.P. Jin. 2005. Proteolytic N-terminal truncation of cardiac troponin I enhances ventricular diastolic function. *J. Biol. Chem.* 280:6602–6609. https://doi.org/10.1074/jbc.M408525200

Bers, D.M., S. Despa, and J. Bossuyt. 2006. Regulation of Ca^{2+} and Na^{+} in normal and failing cardiac myocytes. *Ann. N. Y. Acad. Sci.* 1080:165–177. https://doi.org/10.1196/annals.1380.015

Borlaug, B.A., and D.A. Kass. 2006. Mechanisms of diastolic dysfunction in heart failure. *Trends Cardiovasc. Med.* 16:273–279. https://doi.org/10.1016/j.tcm.2006.05.003

Cazorla, O., A. Freiburg, M. Helmes, T. Centner, M. McNabb, Y. Wu, K. Trombitás, S. Labeit, and H. Granzier. 2000. Differential expression of cardiac titin isoforms and modulation of cellular stiffness. *Circ. Res.* 86: 59–67. https://doi.org/10.1161/01.RES.86.1.59

Chong, S.M., and J.P. Jin. 2009. To investigate protein evolution by detecting suppressed epitope structures. *J. Mol. Evol.* 68:448–460. https://doi.org/10.1007/s00239-009-9202-0

de Tombe, P.P., R.D. Mateja, K. Tachampa, Y. Ait Mou, G.P. Farman, and T.C. Irving. 2010. Myofilament length dependent activation. *J. Mol. Cell. Cardiol.* 48:851–858. https://doi.org/10.1016/j.yjmcc.2009.12.017

Fabiato, A., and F. Fabiato. 1979. Calculator programs for computing the composition of the solutions containing multiple metals and ligands used for experiments in skinned muscle cells. *J. Physiol.* 75:463–505.

Feng, H.Z., B.J. Biesiadecki, Z.B. Yu, M.M. Hossain, and J.P. Jin. 2008a. Restricted N-terminal truncation of cardiac troponin T: A novel mechanism for functional adaptation to energetic crisis. *J. Physiol.* 586: 3537–3550. https://doi.org/10.1113/jphysiol.2008.153577

Feng, H.Z., M. Chen, L.S. Weinstein, and J.P. Jin. 2008b. Removal of the N-terminal extension of cardiac troponin I as a functional compensation for impaired myocardial β-adrenergic signaling. *J. Biol. Chem.* 283: 33384–33393. https://doi.org/10.1074/jbc.M803302200

Feng, H.Z., M.M. Hossain, X.P. Huang, and J.P. Jin. 2009. Myofilament incorporation determines the stoichiometry of troponin I in transgenic expression and the rescue of a null mutation. *Arch. Biochem. Biophys.* 487:36–41. https://doi.org/10.1016/j.abb.2009.05.001

Feng, H.Z., and J.P. Jin. 2010. Coexistence of cardiac troponin T variants reduces heart efficiency. *Am. J. Physiol. Heart Circ. Physiol.* 299:H97–H105. https://doi.org/10.1152/ajpheart.01105.2009

Feng, H.Z., and J.P. Jin. 2020. High efficiency preparation of skinned mouse cardiac muscle strips from cryosections for contractility studies. *Exp. Physiol.* 105:1869–1881. https://doi.org/10.1113/EP088521

Fukuda, N., and H.L. Granzier. 2005. Titin/connectin-based modulation of the Frank-Starling mechanism of the heart. *J. Muscle Res. Cell Motil.* 26: 319–323. https://doi.org/10.1007/s10974-005-9038-1

Gunther, L.K., H.Z. Feng, H. Wei, J. Raupp, J.P. Jin, and T. Sakamoto. 2016. Effect of N-terminal extension of cardiac troponin I on the Ca^{2+} regulation of ATP binding and ADP dissociation of myosin II in native cardiac myofibrils. *Biochemistry*. 55:1887–1897. https://doi.org/10.1021/acs.biochem.5b01059

Hanft, L.M., B.J. Biesiadecki, and K.S. McDonald. 2013. Length dependence of striated muscle force generation is controlled by phosphorylation of cTnI at serines 23/24. *J. Physiol.* 591:4535–4547. https://doi.org/10.1113/jphysiol.2013.258400

Hartzell, H.C., and D.B. Glass. 1984. Phosphorylation of purified cardiac muscle C-protein by purified cAMP-dependent and endogenous Ca^{2+}-calmodulin-dependent protein kinases. *J. Biol. Chem.* 259:15587–15596. https://doi.org/10.1016/S0021-9258(17)42588-9

Huang, X., Y. Pi, K.J. Lee, A.S. Henkel, R.G. Gregg, P.A. Powers, and J.W. Walker. 1999. Cardiac troponin I gene knockout: A mouse model of myocardial troponin I deficiency. *Circ. Res.* 84:1–8. https://doi.org/10.1161/01.RES.84.1.1

Jin, J.P. 1996. Alternative RNA splicing-generated cardiac troponin T isoform switching: A non-heart-restricted genetic programming synchronized in developing cardiac and skeletal muscles. *Biochem. Biophys. Res. Commun.* 225:883–889. https://doi.org/10.1006/bbrc.1996.1267

Kentish, J.C., D.T. McCloskey, J. Layland, S. Palmer, J.M. Leiden, A.F. Martin, and R.J. Solaro. 2001. Phosphorylation of troponin I by protein kinase A accelerates relaxation and crossbridge cycle kinetics in mouse ventricular muscle. *Circ. Res.* 88:1059–1065. https://doi.org/10.1161/hh1001.091640

Kranias, E.G., and R.J. Solaro. 1982. Phosphorylation of troponin I and phospholamban during catecholamine stimulation of rabbit heart. *Nature*. 298:182–184. https://doi.org/10.1038/298182a0

Kumar, M., S. Govindan, M. Zhang, R.J. Khairallah, J.L. Martin, S. Sadayappan, and P.P. de Tombe. 2015. Cardiac myosin-binding protein C and troponin-I phosphorylation independently modulate myofilament length-dependent activation. *J. Biol. Chem.* 290:29241–29249. https://doi.org/10.1074/jbc.M115.686790

Layland, J., R.J. Solaro, and A.M. Shah. 2005. Regulation of cardiac contractile function by troponin I phosphorylation. *Cardiovasc. Res.* 66:12–21. https://doi.org/10.1016/j.cardiores.2004.12.022

Lee, E.J., J. Peng, M. Radke, M. Gotthardt, and H.L. Granzier. 2010. Calcium sensitivity and the Frank-Starling mechanism of the heart are increased in titin N2B region-deficient mice. *J. Mol. Cell. Cardiol.* 49:449–458. https://doi.org/10.1016/j.yjmcc.2010.05.006

LeWinter, M.M., and H.L. Granzier. 2014. Cardiac titin and heart disease. *J. Cardiovasc. Pharmacol.* 63:207–212. https://doi.org/10.1097/FJC.0000000000000007

Li, Y., P.Y. Charles, C. Nan, J.R. Pinto, Y. Wang, J. Liang, G. Wu, J. Tian, H.Z. Feng, J.D. Potter, et al. 2010. Correcting diastolic dysfunction by Ca^{2+} desensitizing troponin in a transgenic mouse model of restrictive cardiomyopathy. *J. Mol. Cell. Cardiol.* 49:402–411. https://doi.org/10.1016/j.yjmcc.2010.04.017

Li, Y., L. Zhang, P.Y. Jean-Charles, C. Nan, G. Chen, J. Tian, J.P. Jin, I.J. Gelb, and X. Huang. 2013. Dose-dependent diastolic dysfunction and early death in a mouse model with cardiac troponin mutations. *J. Mol. Cell. Cardiol.* 62:227–236. https://doi.org/10.1016/j.yjmcc.2013.06.007

Mamidi, R., K.S. Gresham, S. Verma, and J.E. Stelzer. 2016. Cardiac myosin binding protein-C phosphorylation modulates myofilament length-dependent activation. *Front. Physiol.* 7:38. https://doi.org/10.3389/fphys.2016.00038

Martin, A.F. 1981. Turnover of cardiac troponin subunits. Kinetic evidence for a precursor pool of troponin-I. *J. Biol. Chem.* 256:964–968. https://doi.org/10.1016/S0021-9258(19)70073-8

McConnell, B.K., C.S. Moravec, and M. Bond. 1998. Troponin I phosphorylation and myofilament calcium sensitivity during decompensated cardiac hypertrophy. *Am. J. Physiol.* 274:H385–H396. https://doi.org/10.1152/ajpheart.1998.274.2.H385

McConnell, B.K., Z. Popovic, N. Mal, K. Lee, J. Bautista, F. Forudi, R. Schwartzman, J.P. Jin, M. Penn, and M. Bond. 2009. Disruption of protein kinase A interaction with A-kinase-anchoring proteins in the heart in vivo: Effects on cardiac contractility, protein kinase A phosphorylation, and troponin I proteolysis. *J. Biol. Chem.* 284:1583–1592. https://doi.org/10.1074/jbc.M806321200

Rasmussen, M., H.Z. Feng, and J.P. Jin. 2022. Evolution of the N-terminal regulation of cardiac troponin I for heart function of tetrapods: Lungfish presents an example of the emergence of novel submolecular structure to lead the capacity of adaptation. *J. Mol. Evol.* 90:30–43. https://doi.org/10.1007/s00239-021-10039-9

Robertson, S.P., J.D. Johnson, M.J. Holroyde, E.G. Kranias, J.D. Potter, and R.J. Solaro. 1982. The effect of troponin I phosphorylation on the Ca^{2+}-binding properties of the Ca^{2+}-regulatory site of bovine cardiac troponin. *J. Biol. Chem.* 257:260–263. https://doi.org/10.1016/S0021-9258(19)68355-9

Rosas, P.C., Y. Liu, M.I. Abdalla, C.M. Thomas, D.T. Kidwell, G.F. Dusio, D. Mukhopadhyay, R. Kumar, K.M. Baker, B.M. Mitchell, et al. 2015. Phosphorylation of cardiac myosin-binding protein-C is a critical mediator of diastolic function. *Circ. Heart Fail.* 8:582–594. https://doi.org/10.1161/CIRCHEARTFAILURE.114.001550

Schwinger, R.H., M. Böhm, A. Koch, U. Schmidt, I. Morano, H.J. Eissner, P. Uberfuhr, B. Reichart, and E. Erdmann. 1994. The failing human heart is unable to use the Frank-Starling mechanism. *Circ. Res.* 74:959–969. https://doi.org/10.1161/01.RES.74.5.959

Sheng, J.J., and J.P. Jin. 2016. TNNI1, TNNI2 and TNNI3: Evolution, regulation, and protein structure-function relationships. *Gene.* 576:385–394. https://doi.org/10.1016/j.gene.2015.10.052

Shiels, H.A., S.C. Calaghan, and E. White. 2006. The cellular basis for enhanced volume-modulated cardiac output in fish hearts. *J. Gen. Physiol.* 128:37–44. https://doi.org/10.1085/jgp.200609543

Shiels, H.A., and E. White. 2008. The Frank-Starling mechanism in vertebrate cardiac myocytes. *J. Exp. Biol.* 211:2005–2013. https://doi.org/10.1242/jeb.003145

Smith, L., C. Tainter, M. Regnier, and D.A. Martyn. 2009. Cooperative cross-bridge activation of thin filaments contributes to the Frank-Starling mechanism in cardiac muscle. *Biophys. J.* 96:3692–3702. https://doi.org/10.1016/j.bpj.2009.02.018

Subramaniam, A., J. Gulick, J. Neumann, S. Knotts, and J. Robbins. 1993. Transgenic analysis of the thyroid-responsive elements in the α-cardiac myosin heavy chain gene promoter. *J. Biol. Chem.* 268:4331–4336. https://doi.org/10.1016/S0021-9258(18)53614-0

Warren, C.M., P.R. Krzesinski, and M.L. Greaser. 2003. Vertical agarose gel electrophoresis and electroblotting of high-molecular-weight proteins. *Electrophoresis*. 24:1695–1702. https://doi.org/10.1002/elps.200305392

Wei, H., and J.P. Jin. 2015. NH2-terminal truncations of cardiac troponin I and cardiac troponin T produce distinct effects on contractility and calcium homeostasis in adult cardiomyocytes. *Am. J. Physiol. Cell Physiol.* 308: C397–C404. https://doi.org/10.1152/ajpcell.00358.2014

Wolska, B.M., G.M. Arteaga, J.R. Peña, G. Nowak, R.M. Phillips, S. Sahai, P.P. de Tombe, A.F. Martin, E.G. Kranias, and R.J. Solaro. 2002. Expression of slow skeletal troponin I in hearts of phospholamban knockout mice alters the relaxant effect of β-adrenergic stimulation. *Circ. Res.* 90: 882–888. https://doi.org/10.1161/01.RES.0000016962.36404.04

Wu, A.Z., D. Xu, N. Yang, S.F. Lin, P.S. Chen, S.E. Cala, and Z. Chen. 2016. Phospholamban is concentrated in the nuclear envelope of cardiomyocytes and involved in perinuclear/nuclear calcium handling. *J. Mol. Cell. Cardiol.* 100:1–8. https://doi.org/10.1016/j.yjmcc.2016.09.008

Yancy, C.W., M. Jessup, B. Bozkurt, J. Butler, D.E. Casey Jr, M.H. Drazner, G.C. Fonarow, S.A. Geraci, T. Horwich, J.L. Januzzi, et al. 2013. 2013 ACCF/AHA guideline for the management of heart failure: Executive summary: A report of the American College of Cardiology Foundation/American Heart Association Task Force on practice guidelines. *Circulation*. 128:1810–1852. https://doi.org/10.1161/CIR.0b013e31829e8807

Yu, Z.B., L.F. Zhang, and J.P. Jin. 2001. A proteolytic NH2-terminal truncation of cardiac troponin I that is up-regulated in simulated microgravity. *J. Biol. Chem.* 276:15753–15760. https://doi.org/10.1074/jbc.M011048200

Zakhary, D.R., C.S. Moravec, R.W. Stewart, and M. Bond. 1999. Protein kinase A (PKA)-dependent troponin-I phosphorylation and PKA regulatory subunits are decreased in human dilated cardiomyopathy. *Circulation.* 99:505–510. https://doi.org/10.1161/01.CIR.99.4.505

Zhang, R., J. Zhao, A. Mandveno, and J.D. Potter. 1995. Cardiac troponin I phosphorylation increases the rate of cardiac muscle relaxation. *Circ. Res.* 76:1028–1035. https://doi.org/10.1161/01.RES.76.6.1028

Zile, M.R., and D.L. Brutsaert. 2002. New concepts in diastolic dysfunction and diastolic heart failure: Part I: Diagnosis, prognosis, and measurements of diastolic function. *Circulation*. 105:1387–1393. https://doi.org/10.1161/hc1102.105289